

UCLA

UCLA Electronic Theses and Dissertations

Title

Stackable Miniature Fuel Cells with On-Demand Fuel and Oxygen Supply

Permalink

<https://escholarship.org/uc/item/66m5674x>

Author

Hur, Janet

Publication Date

2013

Peer reviewed|Thesis/dissertation

UNIVERSITY OF CALIFORNIA

Los Angeles

Stackable Miniature Fuel Cells
with On-Demand Fuel and Oxygen Supply

A dissertation submitted in partial satisfaction of the
requirements for the degree Doctor of Philosophy
in Mechanical Engineering

by

Janet Hur

2013

© Copyright by

Janet Hur

2013

ABSTRACT OF THE DISSERTATION

Stackable Miniature Fuel Cells
with On-Demand Fuel and Oxygen Supply

by

Janet Hur

Doctor of Philosophy in Mechanical Engineering

University of California, Los Angeles, 2013

Professor Chang-Jin “CJ” Kim, Chair

This dissertation summarizes our progress towards miniature fuel cells that could replace and outperform small batteries to meet various power demands. With increasing need of power being critical for portable electronics, the demand for better batteries continues to grow. Lithium-ion batteries dominate the market at the moment, but the current capacities on the order of 200 Wh/kg are approaching their inherent limits. Many researchers have been pursuing alternative power sources, forming a rapidly growing field in engineering and science. For applications too small for batteries (below 1 cm and even 1 mm), currently no proper power source is available, despite over a decade of significant efforts by many in power micro electromechanical systems (power MEMS). Encouraged by the advantages of their macro counterparts, micro fuel cells have received attention as a potentially powerful, efficient, and clean power source for miniature

applications, resulting in extensive research in micro fuel cells and even commercial introduction of some small fuel cells. However, they are not yet powerful enough to consider someday replacing batteries for a wide range of portable applications. While the promise of fuel cells is in their high theoretical energy density, unfortunately the promise is lost in current portable fuel cells because of their complex system that includes ancillary components such as mechanical pump, reformer, pressurized oxygen source, and gas separator.

This dissertation summarizes our attempt to realize a full (i.e., complete, standalone) fuel cell with small footprint, extending the spirit of self-pumped fuel that eliminated ancillary components in the active fuel circulation system to self-controlled oxygen generation for a packaged oxidant supply. We first eliminate fuel pump, gas separator, membrane electrode assembly (MEA) and even pressurized oxygen tank to make anodic chamber simple and self-regulating. As the next step towards realizing a full fuel cell stackable as batteries, we develop a self-regulating oxygen generation system that supplies oxygen within the fuel cell, i.e., not relying on the ambient air. For our final goal, we integrate the self-pumped fuel supply and the self-regulated oxygen supply into one device to prove the concept of a full fuel cell suitable for a stacked configuration.

The dissertation of Janet Hur is approved.

Pei-Yu Chiou

Bruce S. Dunn

Chih-Ming Ho

Chang-Jin “CJ” Kim, Committee Chair

University of California, Los Angeles

2013

TABLE OF CONTENTS

ABSTRACT OF THE DISSERTATION	ii
TABLE OF CONTENTS	v
LIST OF FIGURES	ix
LIST OF TABLES	xii
ACKNOWLEDGEMENTS	xiii
CHAPTER 1: INTRODUCTION.....	1
1.1 Increasing demands for longer-lasting energy sources	1
1.2 Limitations in currently developed micro power sources.....	2
1.3 Fuel cells as next generation power sources	2
1.4 Limitations in currently developed micro fuel cells	3
1.5 Our solution in development of miniature fuel cells	5
1.6 Overview of this dissertation	7
References.....	8
CHAPTER 2: MEMEBRANELESS FUEL CELLS WITH AIR-BREATHING CATHODE	13
2.1 Introduction.....	13
2.2 Mechanism	14
2.3 Device fabrication.....	17
2.4 Experiment.....	21
2.5 Results and discussion	22
2.5.1 Bubble Pumping	22

2.5.2 Air-breathing Cathode	28
2.5.3 Catalytic Activities.....	29
2.5.4 Polarization Curve	32
2.6 Conclusion	34
References.....	34
CHAPTER 3: MINIATURIZATION OF THE AIR-BREATHING FUEL CELL .	39
3.1 Overall design.....	39
3.2 Fabrication	42
3.3 Catalyst support (Graphite vs. Cr/Au)	45
3.4 Resulting output of the developed micro fuel cell.....	47
Reference	49
CHAPTER 4: OXYGEN GENERATING AND LIMITING CATHODE	51
4.1 Introduction.....	51
4.2 Mechanism.....	55
4.3 Fabrication	56
4.4 Experiment.....	58
4.5 Results and discussion	59
4.5.1 Electrochemical Activity	59
4.5.2 Self-Regulation of O ₂ Bubbles.....	60
4.5.3 Polarization Curve	62
4.6 Conclusion	62
References.....	63
CHAPTER 5: COMBINED FULL FUEL CELL	65

5.1 Introduction.....	65
5.2 Mixed potential issue on oxygen generating plate.....	66
5.3 Mechanism.....	69
5.4 Structure design of hydrogen peroxide DFAFC with self-pumping of fuel.....	69
5.5 Fabrication of designed full fuel cell.....	70
5.6 Experimental setting.....	74
5.7 Testing of integrated fuel cell.....	75
5.7.1 Testing of oxygen generation.....	75
5.7.2 Testing of combined full fuel cell.....	77
5.7.3 OCP of combined full fuel cell.....	78
5.7.4 Performance curve of combined full fuel cell.....	79
5.7.4 Longer pumping of fuel cell.....	80
5.8 Conclusion.....	82
References.....	82
CHAPTER 6: CONCLUSION & OUTLOOK.....	84
6.1 Summary.....	84
6.1.1 Stackable fuel cell.....	85
6.1.2 Balanced anodic and cathodic reaction.....	85
6.1.3 A standalone system of liquid-in-container construction.....	85
6.1.4 High energy density and high power density.....	86
6.1.5 Flexible choice of fuel-electrolyte.....	86
6.1.6 Easy scaling down or scaling up.....	86
6.2 Outlook.....	87

6.2.1 Concentration regulation.....	87
6.2.2 Minimizing catalyst deactivation.....	88
6.2.3 Prototype fuel-cell stack	88
6.2.4 Micromachined smaller fuel cells.....	90
6.2.5 Estimated performance	91
References.....	92

LIST OF FIGURES

Figure 1-1: State-of-art fuel cells from PEM fuel cell (Protonex 100W)	4
Figure 1-2: Conventional microfluidic fuel cell system consisted of ancillary components	5
Figure 1-3: Simplified fuel cell architecture previously developed from our group	6
Figure 2-1: Schematic illustration of bubble pumping mechanism for the proposed self-pumping membraneless fuel cell, shown from the side of the device	17
Figure 2-2: Fabrication of the self-pumping membraneless fuel-cell test device	19
Figure 2-3: (a) SEM of PTFE tape (TaegaSeal), (b) PTFE membrane (Millipore), (c) venting plug in the final device, and (d) venting plug assembly	20
Figure 2-4: Feasibility of employing the bubble-pumping mechanism into laminar-flow-based fuel cells was tested using a dyed fuel	23
Figure 2-5: Snapshots of bubble pumping taken during fuel-cell operation	24
Figure 2-6: Pumping frequency and rate of designed fuel cell	27
Figure 2-7: Comparison of bubble pumping enabled and blocked	28
Figure 2-8: Effect of bubble pumping, moving and venting on cathode electrode	31
Figure 2-9: SEM images of solution-deposited Pd electrocatalyst	32
Figure 2-10: (a) Polarization and (b) power density curves of the device tested using four different HCOOH concentrations and 1 M H ₂ SO ₄ supporting electrolyte	33
Figure 3-1: Further miniaturized fuel cell with microfabricated anode and channel	40
Figure 3-2: Another side view of the micro fuel cell	41
Figure 3-3: Top view of the overlaid channel plate and anode	42

Figure 3-4: Fabrication process flow for micro fuel cells _____	43
Figure 3-5: Photographs taken during fabrication of fuel cell components: anode, channel and cathode _____	44
Figure 3-6: Micro fuel cell assembled into packaging smaller than a thumbnail _____	45
Figure 3-7: Half-cell tests of graphite and Cr/Au catalyst support layers in anolyte ____	46
Figure 3-8: Maximum current density output of microfabricated fuel cell _____	48
Figure 3-9: Pumping effect observed during fuel cell operation _____	49
Figure 4-1: Schematic illustration of components needed in conventional microfluidic fuel cells and the eliminated components in our previous micro fuel cells _____	52
Figure 4-2: Schematic drawing of microstructured cathode _____	56
Figure 4-3: Fabrication of the device _____	57
Figure 4-4: Photographs of fabricated device _____	58
Figure 4-5: Cyclic voltammetry of fabricated cathode _____	60
Figure 4-6: Oxygen bubbles form inside the micro-pockets selectively _____	61
Figure 4-7: Half-cell tests of cathode and anode _____	62
Figure 5-1: Preliminary design of combined full fuel cell _____	67
Figure 5-2: Schematic designs of the full fuel cell combining the self-regulated oxygen supply directly on cathode of self-pumping fuel cell _____	68
Figure 5-3: Process flow to fabricate oxygen generating structure with hydrophilic through holes for slow supply of hydrogen peroxide _____	72
Figure 5-4: Images of fabricated oxygen generating structure _____	72
Figure 5-5: Assembled full fuel cell with self-pumping anode and self-regulated O ₂ supply integrated in one device _____	73

Figure 5-6: Oxygen bubble filling the gap between the oxygen generating structure and a glass slide _____	74
Figure 5-7: Snapshots of rigorous O ₂ generation during testing of oxygen supply ____	76
Figure 5-8: Current density of three different cases of operation _____	78
Figure 5-9: OCP of full fuel cell and air-breathing fuel cells _____	79
Figure 5-10: Polarization curve drawn from the integrated full fuel cell compared with the air-breathing full fuel cell _____	80
Figure 5-11: Fully integrated fuel cell was operated for longer term _____	81
Figure 6-1: Schematic drawing illustrating the proposed fuel cells for stacking _____	90
Figure 6-2: Schematic drawing illustrating the integrated micro fuel cells for stacking	91

LIST OF TABLES

Table 6-1: Comparison of weight and energy capacity between existing batteries and developed fuel cell chips.....	92
---	----

ACKNOWLEDGEMENTS

I would first like to thank my advisor, Professor Chang-Jin Kim, for his guidance, encouragement, and patience. He has not only advised me in research but also taught us graduate students many tools to be successful in academia life. I am also thankful to Professor Bruce Dunn for his valuable comments on my research and his kind suggestions on my career. My appreciation also goes to Professor Chih-Ming Ho and Professor Pei-Yu Chiou for serving in my committee and giving valuable advices.

My former and current colleagues in Micro and Nano Manufacturing Lab have provided me with a friendly environment and encouraging discussions. All the lab members have inspired me and given me generous support and help during my research and dissertation writing. I have always enjoyed their company and have learned a lot from them, during group meetings, in the cleanroom, and sometimes during lab outings and happy hours.

Special thanks to the California NanoSystems Institute (CNSI) for organizing great programs and seminars, especially Materials Creation Training Programs (MCTP) Fellowship. I benefitted from the program not only financially but with great opportunities to do internship, and communicate with other inspiring graduate students in other fields during great courses they provided.

I would also like to express my thanks to my beloved family. My parents, brother and grandparents have always given me their warmest support. And finally my husband, Jangwon, always encouraged and inspired me through the last stage of graduate years.

VITA

August 17, 1984	Born in Paterson, New Jersey
2007	B.S., Mechanical Engineering, Sogang University, Seoul, Korea
2009	Internship, HRL, LLC., Malibu, California
2007 – 2013	Graduate Student Researcher Mechanical and Aerospace Engineering Department University of California, Los Angeles

PUBLICATIONS

- J. I. Hur and C.-J. Kim, “Self-contained oxygen supply for self-regulating miniature fuel cell,” *Proceedings of International Conference on powerMEMS, Atlanta, Georgia, Dec. 2012.*

- J. I. Hur and C.-J. Kim, “A microstructured cathode for fuel cell with self-regulated O₂ bubble creation and consumption,” *Proceedings of IEEE International Conference on Micro Electro Mechanical Systems (MEMS’12)*, Paris, France, Jan. 2012, pp.35-38.
- J. I. Hur, D. D. Meng, and C.-J. Kim, “Self-pumping membraneless miniature fuel cell with an air-breathing fuel-tolerant Pt cathode,” *Journal of Microelectromechanical Systems*, vol. 21 (2), pp. 476-483, 2012.
- G. Sun, J. I. Hur, X. Zhao, and C.-J. Kim, “Fabrication of very-high-aspect-ratio micro metal posts and gratings by photoelectrochemical etching and electroplating,” *Journal of Microelectromechanical Systems*, vol. 20 (4), pp. 876-884, 2011.
- J. I. Hur, D. D. Meng, and C.-J. Kim, “Membraneless micro fuel cell chip enabled by self-pumping of fuel-oxidant mixture,” *Proceedings of International Conference on Micro Electro Mechanical Systems (MEMS’10)*, Hong Kong, China, Jan. 2010, pp. 168-171.
- G. Sun, J. I. Hur, X. Zhao, and C.-J. Kim, “High yield dense array of very-high-aspect-ratio micro metal posts by photo-electrochemical etching of silicon and electroplating with vacuum degassing,” *Proceedings of International Conference on Micro Electro Mechanical Systems (MEMS’10)*, Hong Kong, China, Jan. 2010, pp. 340-343.

CHAPTER 1

INTRODUCTION

1.1 Increasing demands for longer-lasting energy sources

There are increasing need and demand in small power sources with high energy density to supply power to portable consumer electronics, such as cell phones, global positioning systems (GPS), digital cameras, and laptop computers [1-3]. The energy density requirement for portable power sources is ever on the increase. The U.S. military has also had a persistent demand for compact, long-life power sources for meeting the field needs of the soldier [4]. The future-day soldier will be outfitted with high-tech electronics that significantly increase awareness of the combat environment. Radios, night-vision devices, portable computers, and personal cooling systems are all examples of power-hungry devices to be used by the future-day soldier. Also, as micro electromechanical systems (MEMS) technology advanced, various microsystems have become available, such as remote sensors and diagnostic systems, increasing the need of miniature power sources on chip [5-7].

Although there is increasing need in longer-lasting miniature and portable power sources and many efforts have been made in developing micro power sources or power MEMS, proper power sources in miniature scale (below 1 cm and even 1 mm) are yet to be available.

1.2 Limitations in currently developed micro power sources

Researchers have explored many approaches in designing micro power sources, such as micro engines [8, 9], micro batteries [10-12], photovoltaic cells [13-15] and energy harvesting devices [16,17]. Micro engines are designed to draw electrical energy from chemical energy through combustion. However, a practical and standalone system has not become available, hindered mainly by the problems in packaging and thermal management due to the high temperature and high pressure required for operation, both inherently disadvantageous with miniaturization. Batteries are attractive and commonly chosen in centimeter scales. However, in millimeter scale it is not practical due to the limited energy storage capacity in a small volume. Energy harvesting devices have been sought to collect power from the environment in the form of mechanical vibration, electromagnetic wave, or thermal energy. However, the uncertainty and low amplitude nature of environmental energy require additional components to properly convert and store the harvested energy.

1.3 Fuel cells as next generation power sources

Being environmentally friendly, fuel cells are attractive in both macro and micro scales. Especially in microscale, the simple construction compared to internal combustion engines and high theoretical energy density compared to batteries make fuel cells a strong candidate. Miniature fuel cells, based on direct methanol fuel cell (DMFC) technology [18-20] and direct formic acid fuel cell (DFAFC) [21-23], have been actively reported using a membrane electrode assembly (MEA) [24] or a membraneless technique [25-29]. Moreover, the U.S. Department of Transportation has approved the use of some fuel cells

in airplanes, removing what companies have called a major barrier keeping micro fuel cells out of electronic devices such as laptops and cell phones [30].

1.4 Limitations in currently developed micro fuel cells

Although many have reported fuel cells well shrunk in size and named them micro fuel cells, almost all of them are micro fuel-cell stack, not a micro fuel cell complete as a standalone system. To form a complete system, the micro fuel-cell stacks are still attached to bulky ancillary components. In other words, they require a pump to flow the liquid fuel and to force the flow against carbon dioxide bubble clogging, a gas separator to remove the bubbles, and often a pressurized oxygen tank to deliver oxygen to the system.

Current state-of-art fuel cells from proton exchange membrane (PEM) fuel cell from Protonex, shown in Figure 1-1, consist of several ancillary components [30-31]. Further miniaturization and packaging is complicated since these supporting components take up significant portion of the total volume posing limitation in miniaturization. The schematic drawing of the components needed in conventional miniature fuel cells is shown in Figure 1-2.

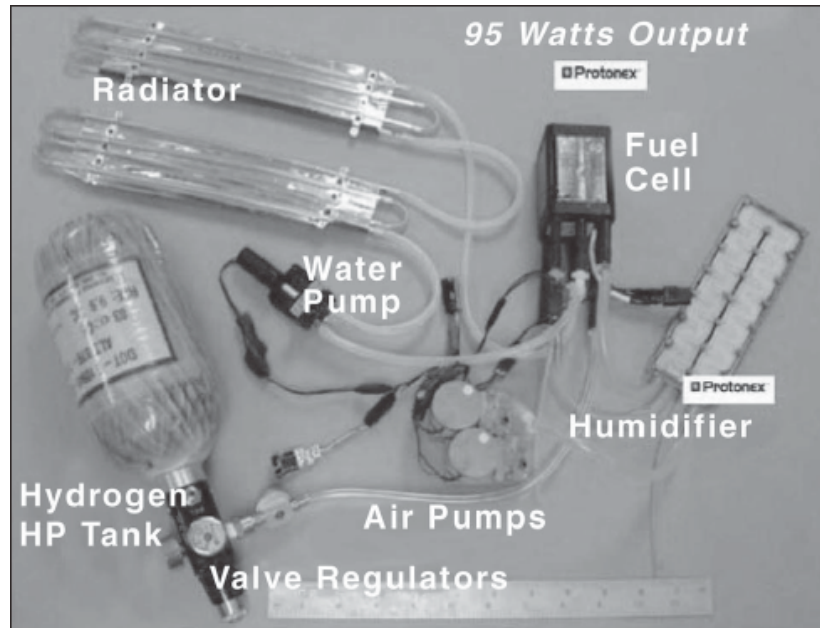


Figure 1-1: State-of-art fuel cells from PEM fuel cell (Protonex 100W). Conventional microfluidic fuel cell system consisted of ancillary components. In a miniaturized configuration, these supporting components take up significant portion of the total volume posing limitation in miniaturization [30].

Only after all these ancillary components are connected to the micro fuel cell stack, one will have a system that functions as a fuel cell. Unfortunately, when the supporting structures are miniaturized as much as possible (note: no suitable micro pump is available even today) and integrated into the system, the inactive (i.e., non-fuel) materials take up a considerable volume of fuel cell—the so-called “packaging penalty,” reducing the fuel and oxidant storage capacity. With the above common miniaturization approach, the packaging penalty becomes unacceptably high if a fuel cell (again, not fuel-cell stack) should be below 1 cm in size – the main reason the flurry of activities in micro fuel cells subsided after early 2000s.

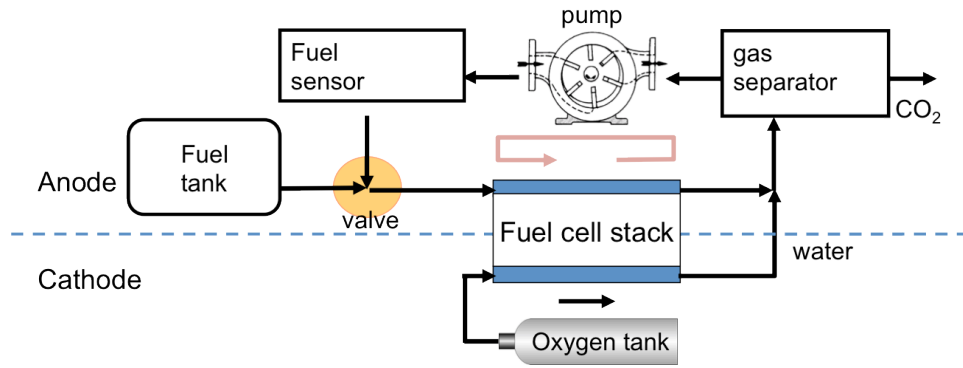


Figure 1-2: Conventional microfluidic fuel cell system consisted of ancillary components. In a miniaturized configuration, these supporting components take up significant portion of the total volume posing limitation in miniaturization.

1.5 Our solution in development of miniature fuel cells

The difficulty in miniaturizing and packaging the ancillary components (e.g., pumps, regulators) hindered fuel cells from becoming a compact product to compete with batteries. The inactive ancillary components would occupy a significant volume in the fuel cell – the so-called “packaging penalty,” reducing the volume for active fluids (e.g., fuel and oxidant). With only a small amount of active fluids in the system, the advantage of high energy density is simply lost in a complete (i.e., full, standalone) fuel cell. Furthermore, the complexity of integrating the moving ancillary components would make the miniature system expensive and unreliable.

We have previously reported a self-pumping fuel cell that has an embedded ability to pump the liquid fuel and separate the gas phase, allowing one to miniaturize fuel cells (at least the anodic side) without the packaging penalty [32-34]. Unlike other passive fuel cells [19, 23, 35], the self-pumping fuel cell actively pumps to deliver fresh

fuel from a reservoir, where fuel concentration is kept constant. Utilizing the carbon dioxide byproduct on anode was the key idea for this device. Directionally growing bubbles from the inlet and venting them out through the outlet pumped the fuel in the same direction as the microfluidic channel. Doing so enabled us to eliminate the mechanical pump and gas separator altogether (Fig. 1-3). This method is applicable and flexible to any kind of fuel, as long as the fuel produces carbon dioxide as byproduct on anode. However, the cathode was still attached to a pressurized oxygen tank to supply enough oxygen for a balanced anode and cathode reaction.

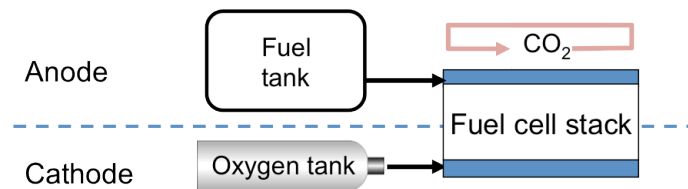


Figure 1-3: Simplified fuel cell architecture previously developed from our group [32].

Once the anodic channel has been compactly designed with bubble pumping and gas venting, the next problem against obtaining a miniature fuel cell was lack of a proper oxygen supply on the cathode side. In order to eliminate an oxygen tank, people have attempted to flow an oxygen-saturated oxidant inside the cathodic channel [26, 27] or settled with an air-breathing cathode [19-21, 25] supplied of oxygen from ambient air. We report a microstructure, which if electrified in a hydrogen peroxide solution covers its top with a thin layer of oxygen gas in a self-regulating manner. In pursuit of realizing a full fuel cell with no moving part, we have successfully developed such an oxygen-generating surface and integrated it as a direct oxygen supply to the cathode of our

previously developed miniature fuel cells. The resulting fuel cell showed a significant increase in current density, compared with the previous air-breathing counterpart. This unique oxygen supply takes up a much smaller volume than the existing designs, which require ancillary components, such as a pressurized oxygen tank with a regulator. In designing a fully functional (i.e., self-sustainable) miniature fuel cell, elimination of the need to access the ambient air allows a stackable configuration of multiple fuel cells for higher power demands.

Developed technologies can reduce the total weight of power supply carried by individuals or even small unit soldiers without degrading the power capacity. Because of the high specific energy density, our eventual fuel cells are expected to weigh between 1/8 and 1/2 of the current Li-ion batteries. Furthermore, the reported research is directly related to advancing technology in renewable energy to reduce the world's dependence on fossil fuel.

1.6 Overview of this dissertation

In this report, we introduce our novel ways to further miniaturize the fuel cell system and continuous effort towards stackable unit fuel cells. In Chapter 2, we will introduce that the entire ancillary components (even the MEA) can be eliminated from a complete fuel cell, by providing the fuel via the self-pumping mechanism and oxygen via air breathing. Chapter 3 describes our effort to further miniaturize the air-breathing fuel cell into microscale fuel cell system. In Chapter 4, we will introduce our approach to solve the oxygen deficiency in stackable fuel cells. Finally, in Chapter 5, presented is

how we combine both of the technologies described in Chapters 2 and 4 to realize a full fuel cell with self-regulated fuel and oxygen supply in a simple architecture.

References

- [1] P. Somavat and V. Namboodiri, “Energy consumption of personal computing including portable communication devices,” *Journal of Green Engineering*, pp. 447–475, 2011.
- [2] M. Yunt, B. Chachuat, A. Mitsos, and P. I. Barton, “Designing man-portable power generation systems for varying power demand,” *American Institute of Chemical Engineers*, vol. 54, pp. 1254-1269, 2008.
- [3] B. R. Chalamala, “Portable electronics and the widening energy gap,” *Proceedings of IEEE*, vol. 95, pp. 2106-2107, 2007.
- [4] S. R. Narayan and T. I. Valdez, “High-energy portable fuel cell power sources,” *The Electrochemical Society Interface*, pp. 40-45, 2008.
- [5] D. Schubert, “MEMS-concept using micro turbines for satellite power supply,” *InTech*, pp. 195-210, 2012.
- [6] F. Beyeler, S. Muntwyler, Z. Nagy, C. Graetzel, M. Moser and B. J. Nelson, “Design and calibration of a MEMS sensor for measuring the force and torque acting on a magnetic microrobot,” *J. Micromech. Microeng.*, vol. 18, pp.1-7, 2008.
- [7] N. K. S. Lee, R. S. Goonetilleke, Y. S. Cheung, and G. M. Y. So, “A flexible encapsulated MEMS pressure sensor system for biomechanical applications,” *Microsystem Technologies*, vol. 7, pp. 55-62, 2001.

- [8] J. Knobloch, M. Wasilik, A. C. Fernandez-Pello, and A. P. Pisano, "Micro, internal-combustion engine fabrication with 900 mm deep features via DRIE," *Proc. 2003 Int. Mechanical Engineering Congress and Exposition (IMECE), Washington D.C., Nov. 2003*.
- [9] M. K. Senesky and S. R. Sanders, "A millimeter-scale electric generator," *IEEE Trans. Ind. Appl.*, vol. 44, pp. 1143-1149, 2008.
- [10] J. W. Long, B. Dunn, D. R. Rolison, and H. S. White, "Three-dimensional battery architectures," *Chem. Rev.*, vol. 104, pp. 4463-4492, 2004.
- [11] N. J. Dudney, "Thin film micro-batteries," *The Electrochemical Society Interface*, pp. 44-48, 2008.
- [12] M. S. Park, G. X. Wang, H. K. Liu, and S. X. Dou, "Electrochemical properties of Si thin film prepared by pulsed laser deposition for lithium ion micro-batteries," *Electrochimica Acta*, vol. 51, pp. 5246-5249, 2006.
- [13] Z. Li, G. He, X. Wan, Y. Liu, J. Zhou, G. Long, Y. Zuo, M. Zhang, and Y. Chen, "Solution Processable Rhodanine-Based Small Molecule Organic Photovoltaic Cells with a Power Conversion Efficiency of 6.1%," *Advanced Energy Materials*, vol. 2, pp. 74-77, 2012.
- [14] W.-H. Lee, S. K. Son, K. Kim, S. K. Lee, W. S. Shin, S.-J. Moon, and I.-N. Kang, "Synthesis and Characterization of New Selenophene-Based Donor-Acceptor Low-Bandgap Polymers for Organic Photovoltaic Cells," *Macromolecules*, vol. 45, pp. 1303-1312, 2012.
- [15] M. Gratzel, "Solar energy conversion by dye-sensitized photovoltaic cells," *Inorganic Chemistry*, vol. 20, pp. 6841-6851, 2005.

- [16] J. S. Boland, J. D. M. Messenger, H. W. Lo, and Y. C. Tai, "Arrayed liquid rotor electret power generator systems," *18th IEEE International Conference on Micro Electro Mechanical Systems (MEMS 2005)*, pp. 618-621, 2005.
- [17] S. Boisseau, G. Depesse, and A. Sylvestre, "Optimization of an electret-based energy harvester," *Smart Mater. Struct.*, vol. 19, p. 10pp, 2010.
- [18] T. Hottinen, M. Mikkola, and P. Lund, "Evaluation of planar free-breathing polymer electrolyte membrane fuel cell design," *J. Power Sources*, vol. 129, pp. 68-72, 2004.
- [19] T. Shimizu, T. Momma, M. Mohamedi, T. Osaka, and S. Sarangapani, "Design and fabrication of pumpless small direct methanol fuel cells for portable applications," *J. Power Sources*, vol. 137, pp. 277-283, 2004.
- [20] C. Y. Chen and P. Yang, "Performance of an air-breathing direct methanol fuel cell," *J. Power Sources*, vol. 123, pp. 37-42, 2003.
- [21] S. Ha, B. Adams, and R. I. Masel, "A miniature air breathing direct formic acid fuel cell," *J. Power Sources*, vol. 128, pp. 119-124, 2004.
- [22] C. Rice, S. Ha, R. I. Masel, P. Waszczuk, A. Wieckowski, and T. Barnrad, "Direct formic acid fuel cells," *J. Power Sources*, vol. 111, pp. 83-89, 2002.
- [23] J. Yeom, R. S. Jayashree, C. Rastogi, M. A. Shannon, and P. J. A. Kenis, "Passive direct formic acid microfabricated fuel cells," *J. Power Sources*, vol. 160, pp. 1058-1064, 2006.
- [24] G. Q. Lu, C. Y. Wang, T. J. Yen, and X. Zhang, "Development and characterization of a silicon-based micro direct methanol fuel cell," *Electrochimica Acta*, vol. 49, pp. 821-828, 2004.

- [25] R. S. Jayashree, L. Ganes, E. R. Choban, A. Primak, D. Natarajan, L. J. Markoski, and P. J. A. Kenis, "Air-breathing laminar flow-based microfluidic fuel cell," *J. Am. Chem. Soc.*, vol. 127, pp. 16758-16759, 2005.
- [26] J. L. Cohen, D. J. Volpe, D. A. Westly, A. Pechenik, and H. D. Abruna, "A dual electrolyte H₂/O₂ Planar membraneless microchannel fuel cell system with open circuit potentials in excess of 1.4 V," *Langmuir*, vol. 21, pp. 3544-3550, 2005.
- [27] E. R. Choban, L. J. Markoski, A. Wieckowski, and P. J. A. Kenis, "Microfluidic fuel cell based on laminar flow," *J. Power Sources*, vol. 128, pp. 54-60, 2004.
- [28] R. Ferringo, A. D. Stroock, T. D. Clark, M. Mayer, and G. M. Whitesides, "Membraneless vanadium redox fuel cell using laminar flow," *J. Am. Chem. Soc.*, vol. 124, pp. 12930-12931, 2002.
- [29] E. Kjeang, A. G. Brolo, D. A. Harrington, N. Djilali, and D. Sinton, "Hydrogen peroxide as an oxidant for microfluidic fuel cells," *J. Electrochem. Soc.*, vol. 154, pp. B1220-B1226, 2007.
- [30] <http://www.greentechmedia.com/articles/read/will-micro-fuel-cells-fly-high-855>.
- [31] V. P. McConnell, "Military UAVs claiming the skies with fuel cell power," *Fuel Cells Bulletin*, vol. 2007, pp. 12-15, 2007.
- [32] D. D. Meng and C.-J. Kim, "An active micro-direct methanol fuel cell with self-circulation of fuel and built-in removal of CO₂ bubbles," *J. Power Sources*, vol. 194, pp. 445-450, 2009.
- [33] J. I. Hur, D. D. Meng, and C.-J. Kim, "Self-Pumping Membraneless Miniature Fuel Cell with an Air-breathing Fuel-Tolerant Pt Cathode," *J. MEMS*, Vol. 21, 2012, pp. 476-483.

- [34] J. I. Hur and C.-J. Kim, "A microstructured cathode for fuel cell with self-regulated O₂ bubble creation and consumption," *25th IEEE International Conference on Micro Electro Mechanical Systems (MEMS 2012)*, pp. 35-38, 2012.
- [34] J. G. Liu, T. S. Zhao, R. Chen, and C. W. Wong, "The effect of methanol concentration on the performance of a passive DMFC," *Electrochem. Commun.*, vol. 7, pp. 288-294, 2005.
- [35] E. Kjeang, B. T. Proctor, A. G. Brolo, D. A. Harrington, N. Djilali, and D. Sinton, "High-performance microfluidic vanadium redox fuel cell," *Electrochimica Acta*, vol. 52, pp. 4942-4946, 2007.

CHAPTER 2

MEMEBRANELESS FUEL CELLS

WITH AIR-BREATHING CATHODE

2.1 Introduction

While the self-pumping mechanism dramatically simplified the anode side as described in the previous chapter, the oxygen source for the cathode side still remains as a bulky attachment in the form of a pressurized oxygen tank, a fan or microchannels filled with actively-pumped, oxygen-saturated electrolyte solution. An air-breathing cathode is acceptable for some cases of both direct methanol fuel cell (DMFC) [1-3] and direct formic acid fuel cell (DFAFC) [4-6]. Oxygen from ambient air is readily supplied to the air-breathing cathode, which is practical if the system allows enough free convection of air. However, the performance of the whole system may seriously suffer if the oxygen supply is hindered by water flooding or limited area open to air, especially when high current density is drawn [7, 8]. Although an air-breathing cathode bears problems stated above, when designed carefully it is an attractive method to replace the bulky oxygen tank.

Aiming to provide a systematic solution for micro fuel cells with the self-pumping mechanism, in this chapter we focus on the elimination of the membrane electrode assembly (MEA), which has usually been regarded as an essential component of most low-temperature fuel cells. However, the two-compartment configuration, separated by an MEA, is closely associated with many problems of fuel-cell systems, including fuel

crossover, cathode flooding, anode drying out, and difficulty in miniaturization and integration with MEMS devices [9]. Recently, microfluidic membraneless fuel cells have been developed that flow two laminar streams of fuel and oxidant side by side to establish a virtual proton exchange membrane, thus eliminating the physical MEA and significantly reducing the above-discussed problems [10-16]. Alternatively, the MEA can be eliminated from a fuel-cell system by flowing a mixed reactant into reaction site consisted of selective catalysts [17-22], for which case the design of fuel cell is extremely simplified. While these methods eliminate the need of an MEA, an external pump is still necessary to deliver the fuel into the reaction channel. Laminar-flow-based fuel cells especially need active fuel pumping with certain flow rates to maintain the laminar interface between the fuel and oxidant streams [23].

In this chapter, we report an active fuel cell that uses neither an MEA nor ancillary parts by implementing the self-pumping mechanism into the membraneless design for their synergic advantages. The concept of this new architecture is proven by successfully demonstrating a self-standing miniature fuel cell and confirming its power-generating capability. Consisting of only solid-state structures with no moving parts, the simple system not only helps constructing miniature fuel cells but also shows a potential for scalable design and manufacturing, which may lead to regular-scale systems as well.

2.2 Mechanism

By embedding the bubble-driven micro pumping mechanism [25] into fuel-cell microchannels, Meng and Kim [26] utilized the CO₂ bubbles formed inside the reaction microchannels to pump the fuel. An abrupt change in the inner diameter of the channel,

called a “virtual check valve”, was placed at the entrance of the channel to block the bubble from growing toward the fuel inlet, and thus directed the bubble to grow only toward the outlet. After expanding to reach the nanoporous hydrophobic venting membrane, the CO₂ was removed through the numerous pores in the venting membrane [27], completing one pumping pulse and starting the next. The result was a directional pumping and circulation of the fuel, as confirmed with an MEA-based micro DMFC [26].

Since the bubble pumping action tends to disrupt the flows and mix the fluid inside the channel, instead of employing laminar-flow-based fuel cell, we considered flowing a single stream of pre-mixed fuel and electrolyte as a better platform to design membraneless self-pumping fuel cells. Unlike other mixed-reactant fuel cells where fuel and oxidant are mixed, oxygen is supplied through an air-breathing cathode to the catalyst-electrolyte interface in order to eliminate oxygen deficiency as a factor in developing the new architecture. Generally, when flowing a mixed stream, the anode and cathode catalysts should selectively oxidize the fuel and reduce the oxygen, respectively. Platinum is known to be one of the preferred catalysts for both fuel oxidation and oxygen reduction. However, platinum has not been considered as a preferable catalyst for the cathode of mixed-reactant fuel cells due to the severe mixed potential. As a result, other fuel tolerant materials with inferior catalytic activities (e.g., non-noble metals) are commonly used as the cathode catalysts. Interestingly, however, we have found that the platinum is fuel tolerant in our design, allowing us to use platinum for the cathode catalyst. This unexpected but welcome discovery is discussed later in *Section 2.5 Results and Discussion*. While Pt is used as the catalyst on the cathode, Pd on the anode provides

an initial selectivity in the mixed reactant situation. Pd is also a better catalyst in DFAFC [28].

The schematic illustration in Fig. 2-1 describes the working mechanism of a membraneless self-pumping fuel cell proposed and developed in this paper. First, the reactant channel is filled with a fuel-electrolyte mixture. When the two fuel-cell electrodes (anode and cathode) are connected through an electrical load, the electrocatalytic reaction starts to generate power, producing CO₂ as a byproduct. The CO₂ nucleates on the anode catalyst as bubbles start to grow, as shown in Fig. 2-1(a). Soon the bubbles merge into a large bubble, which grows rightward because the virtual check valve blocks the leftward growth, pushing the liquid towards the outlet, as illustrated in Fig. 2-1(b). During the process, the large bubble collects and clears most of the bubbles in the reaction channel. After growing to reach the venting membrane, as described in Fig. 2-1(c), the bubble is removed rapidly through the hydrophobic nanoporous membrane. While the bubble shrinks (by venting), fresh fuel is pulled in, starting a new cycle of reaction and pumping, as illustrated in Fig. 2-1(d). Because the bubble starts to appear first near the check valve, the size of the bubble is larger on the left inside the reaction channel within a pumping cycle. The bubble right next to the check valve is always the largest, minimizing the backflow and keeping the self-pumping mechanism inherently efficient.

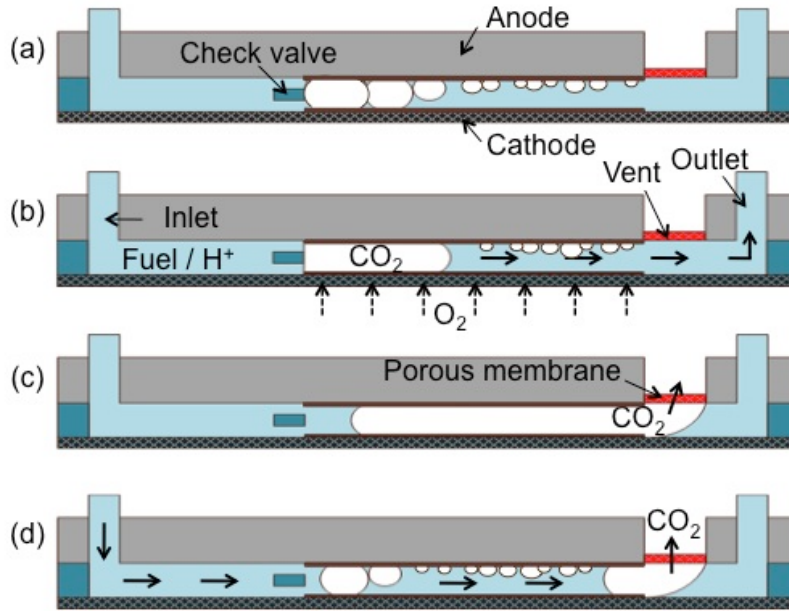


Figure 2-1: Schematic illustration of bubble pumping mechanism for the proposed self-pumping membraneless fuel cell, shown from the side of the device. (a) A mixed stream of fuel and electrolyte starts the reaction on each electrode, creating CO₂ bubbles inside the channel. (b) As the bubbles grow, they merge into a single large bubble. Further growth of the bubble is blocked by the check valve near the inlet forcing the bubble to propagate to the right inside the reaction channel. This process pushes the used fuel stream out to the outlet. (c) When the bubble grows long enough to reach the porous membrane, only gas vents through the membrane. (d) As the bubble shrinks due to the venting, fresh fuel is streamed into the channel, starting the next pumping cycle.

2.3 Device fabrication

Figure 2-2 shows the device we developed to test the concept of mixed-reactant self-pumping fuel cell. Anode was made of 5 mm thick graphite plate (EDM Supplies Inc.) cut into 75 mm in length and 20 mm in width. Three holes of 5 mm in diameter

were drilled to form inlet, outlet and gas vent. After the machining is done, the graphite plate is rinsed with methanol and sonicated in a water bath to remove the debris and particles generated during the machining. A Pd catalyst ink was dropped and dried to cover the reaction area, loading 2 mg/cm^2 of Pd black on the graphite plate. A channel plate was made by cutting the channel shape out from a 1.6 mm thick clear PMMA sheet using the Prolight[®] CNC milling machine. A check valve was designed into the channel (see the magnified figure in the inset) to block the bubble growth. The channel was configured in a diverging shape so that the built-in pressure difference between the left and right meniscus of the bubbles in the channel helps the medium-size bubbles move toward the outlet even before the large bubble is formed and directed by the check valve. The sidewalls of the channel were made transparent by polishing the surface with grade 1500 sandpaper and a polishing compound (Turtle Wax[®]) to allow visual observation of the bubble pumping process during experiments. In the device demonstrated here, cathode was made of a carbon cloth with 0.5 mg/cm^2 using 30 wt% Pt on Vulcan XC-72. A Pt catalyst ink was dropped and dried, loading 2 mg/cm^2 of additional Pt black on the reaction area. The prepared carbon cloth served as air-breathing cathode to use a high oxygen supply from the ambient air rather than relying on the oxygen dissolved in the fuel-oxidant mixture in conventional mixed-reactant fuel cells.

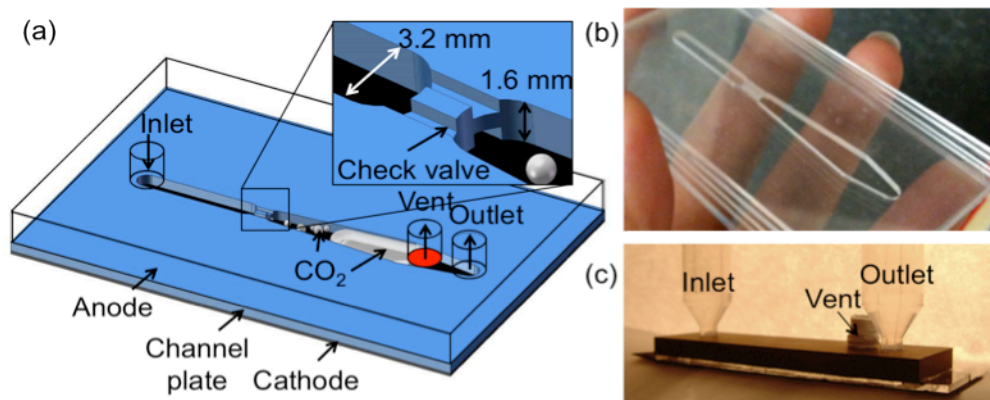


Figure 2-2: Fabrication of the self-pumping membraneless fuel-cell test device. (a) Schematic showing three parts: anode, channel plate, and cathode. The graphite anode, drawn transparent, has three drilled holes for liquid inlet, outlet and gas vent. The channel plate, CNC-machined out of a PMMA and drawn in bright blue, defines the microchannel shape and provides the virtual check valve. The thin dark blue plate on the bottom is an air-breathing cathode. (b) The fabricated transparent channel plate, and (c) the final assembled device with reservoirs used for visualizing fuel delivery.

Catalyst ink was prepared by measuring out a proper amount of Pd black or Pt black particles and adding 10 wt% Nafion[®] solution (Dupont) for proton conduction and particle binding. For each case, deionized water was added to make the total volume 500 μL . Then we metered a droplet volume to deposit 2 mg of Pd and 1 mg of Nafion per square centimeter for the anode catalyst ink or 2 mg of Pt and 0.1 mg of Nafion per square centimeter for the cathode catalyst ink. After dropping and spreading the catalyst ink on the corresponding electrode, the solvent was evaporated under room temperature. Loading of Pd or Pt black was determined to be 2 mg/cm^2 , to prevent the catalyst layer from building internal stress and peel off from the electrode. When ready, the anode and the channel plate were glued with rubber cement and the channel plate and the cathode

with epoxy to assemble the device. Rubber cement allowed us to disassemble the anode for modifications, while epoxy provided a strong bonding for the flexible cathode against leaking. Both rubber cement and epoxy are not directly exposed to the fuel stream unless the contamination from smeared electrolyte in the gap in the assembled device diffuses out to the main stream. So far there has been no noticeable degradation after testing. We used a polytetrafluoroethylene (PTFE) tape, commonly known as “Teflon tape,” which is widely available as a sealing material. Compared with the PTFE membrane from Millipore used in preceding work [25], the Teflon tape has a similar pore diameter as seen in Fig. 2-3(a) and (b). When used in our fuel cell, it properly vented out the CO₂ bubble without leakage. When plugging the venting hole, Teflon tape can seal around the hole without any other sealant.

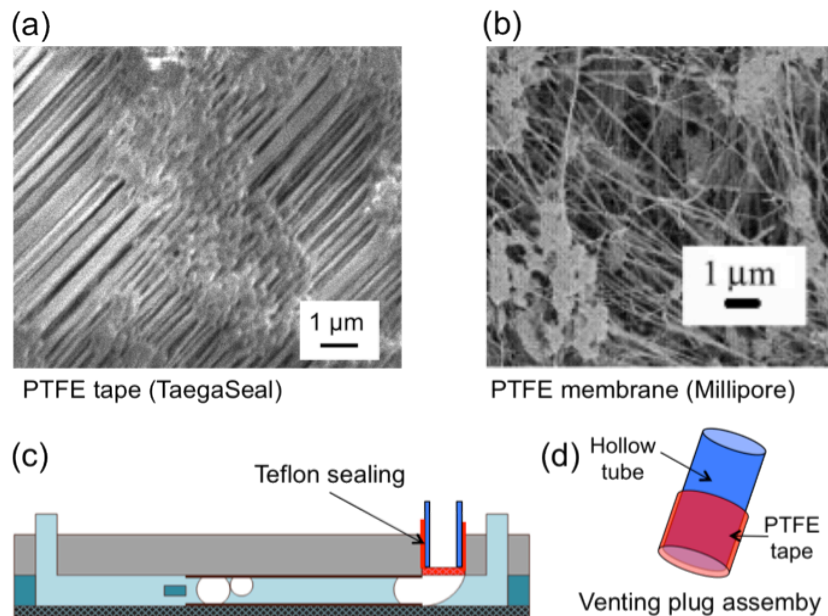
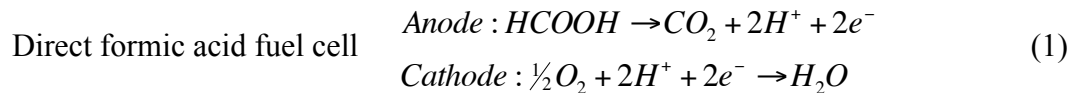


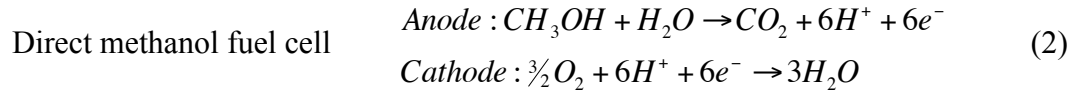
Figure 2-3: (a) SEM of PTFE tape (TaegaSeal) and (b) PTFE membrane (Millipore). Although PTFE tape (TaegaSeal) has more directional pore patterns, they both have pore sizes in the order of 100 nm. (c) In the final device, venting plug assembly is plugged into the venting hole. PTFE tape wrapped around a hollow tube gives air-tight

sealing, and (d) hollow tube of venting plug assembly gives a structural support to the PTFE venting membrane.

2.4 Experiment

The reported membraneless self-pumping fuel cell developed above has been characterized with a potentiostat/galvanostat Model 263A (Princeton Applied Research). Our presented data is normalized with respect to the cathodic catalyst-exposed area of 1.0 cm², while the area of anode catalyst is smaller (0.78 cm²) due to the venting hole, to maintain a conservative view. The device was clamped and held in the air for sufficient oxygen supply under room temperature and ambient pressure. The fuel solution was filled into the inlet tubing, and the waste flowed into the outlet tubing. Reservoirs with a large area were connected to inlet and outlet through tubing and placed on the same level to avoid hydraulic pressure build up or gravity driven fuel delivery during regular fuel cell testing. To confirm fuel delivery easily, however, reservoirs with a small area were placed above the inlet and outlet (Fig. 4c). One can monitor the fuel delivery simply by reading the levels in the reservoirs. The solution was prepared by mixing various concentrations (0.5M, 1M, 5M, 10M) of formic acid (HCOOH, Sigma-Aldrich) into 1M sulfuric acid (H₂SO₄, EMD), which is fuel and electrolyte respectively. Here, formic acid was used as the fuel, since more CO₂ bubbles are produced for a given current output, compared with direct methanol fuel cell [29], as shown below.





Diluted sulfuric acid is used as an electrolyte for proton conduction through the liquid inside the channel. At the same time, it serves as the medium for oxygen to diffuse from ambient air into the vicinity of the cathode. Bubble pumping was recorded with a digital camera from the side of the device through the transparent channel plate.

2.5 Results and discussion

2.5.1 Bubble Pumping

Before employing the reported architecture to eliminate MEA, we have concluded applying the bubble pumping mechanism to the membraneless microfluidic fuel cell of fuel-oxidant laminar streams is impractical at this point. To evaluate the feasibility, we have tested the effect of moving bubbles, as shown in Fig. 2-4, by flowing a dyed water stream laminarily in parallel with a dye-free water stream. Then, bubbles were injected into the channel by a syringe to mimic the bubble pumping of the self-pumping fuel cell. After a few cycles of bubble injection and venting, however, the two streams were found to be mixed. Although it may be possible to minimize the disruption of the laminar flows by design optimization eventually, we decided to employ a mixed-reactant fuel cell approach in our system.

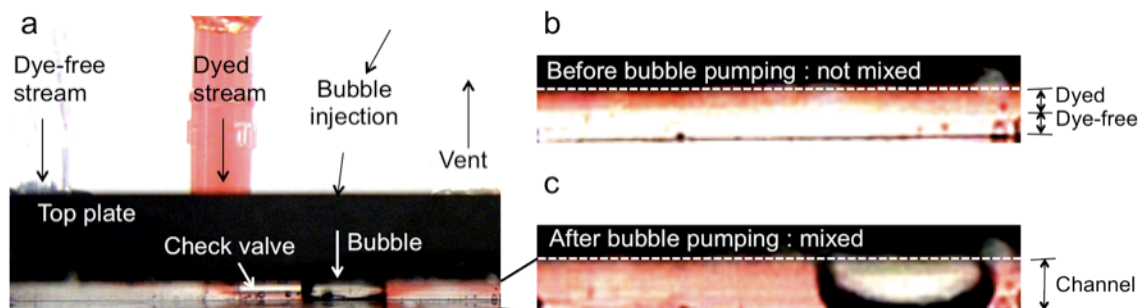


Figure 2-4: Feasibility of employing the bubble-pumping mechanism into laminar-flow-based fuel cells was tested using a dyed fuel. (a) After pumping a dyed stream (red) and dye-free stream (clear) through the top plate (shown black) into the microchannel to establish a laminar interface, we injected bubbles with a syringe into the right end of the valve. (b) Before the bubble pumping, the dyed stream flows parallel to the dye-free stream without mixing. (c) After few cycles of bubble pumping, the two streams are found mixed. Please see the colored version for clarity.

Different from the normal fuel-cell testing conditions, a setup with individual reservoirs above the inlet and outlet was used for an easy visual confirmation of fuel delivery. A successful bubble pumping would deliver the fuel from the inlet to outlet and make the level of the fuel reservoir fall and that of the waste rise. The pumping action inside the channel was visually observed from the side through the transparent channel plate. Some snap shots of the video recordings are presented in Fig. 2-5, which confirms that the CO₂ bubbles grow directionally to the right toward the venting site (Figs. 2-5(a) and (b)). As the large bubble leaves the channel through the venting membrane and a fresh fuel enters the reaction channel from the left, new small bubbles start to nucleate near the entrance (Figs. 2-5(c) and (d)), starting a new pumping cycle, as designed in Fig. 2-4. At the same time, we observed that the liquid level of the waste reservoir above the

outlet rose and the level of the fuel reservoir above the inlet fell, when bubble reached venting membrane and left the channel. On the other hand, the level in fuel reservoir maintained its level while bubble was growing, confirming that the CO₂ bubbles generated by the fuel-cell electrochemistry indeed pump the fuel mixture across the channel. However, the setup in this experiment, designed particularly to prove the concept with a focus on visual confirmation of the self-pumping mechanism, is not capable of operating as a fuel cell for long, because the hydraulic backpressure eventually grows too high to pump against. Although the fuel is delivered by surface tension and in essence not sensitive to gravitational orientation, the device in this experimental setup is affected by the hydraulic pressure; note the fuel column falls and the waste column rises as the fuel is consumed. These columns are made open to air and placed vertical in this experiment to confirm the proposed device can pump against a backpressure. In real practice, a complete fuel-cell system will be designed so that the fuel cartridge is slightly pressurized or balanced with the waste side.

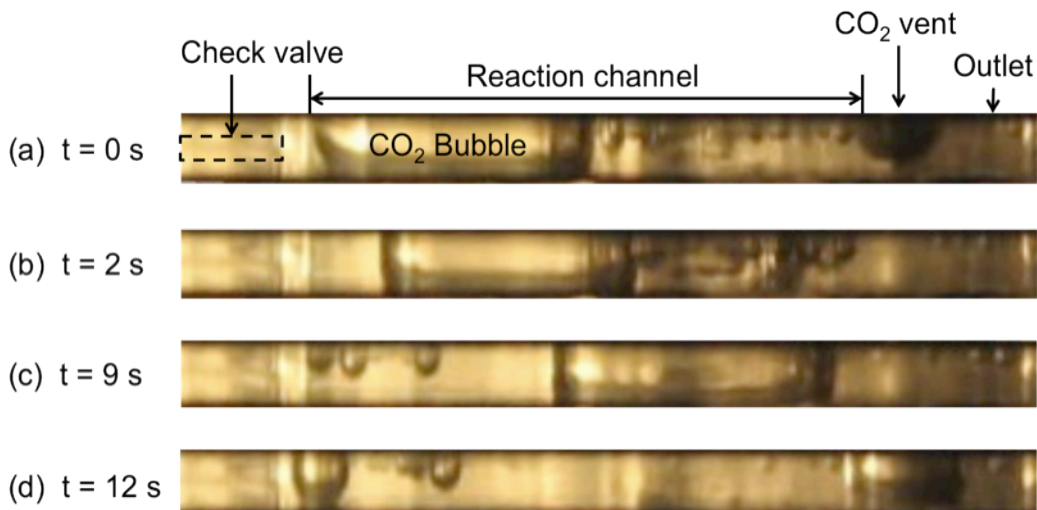


Figure 2-5: Snapshots of bubble pumping taken during fuel-cell operation. 1 M formic acid was used as fuel mixed in 1M sulfuric acid under ambient pressure and room

temperature. CO₂ bubbles successfully nucleated, grew, merged, moved along the diverging channel, and vented out of the channel through the hydrophobic nanoporous membrane.

In order to theoretically assess the capability of the reported method to supply enough fuel for the reaction, we estimated the rate at which the microchannel can be refreshed at certain electrical current output. To simplify the analysis, we assume that the large CO₂ bubble fills up the entire reaction channel (between the check valve and the gas vent). The number of CO₂ molecules needed to fill up the channel is estimated using the ideal gas law under standard conditions for temperature and pressure (STP).

$$PV = nRT \quad (3)$$

where P is the absolute pressure of the gas, V is the volume of the gas, n is number of moles, R is the universal gas constant, and T is the absolute temperature. Since two electrons need to flow from anode to cathode to produce one molecule of CO₂, it is calculated that the present test device (the geometries given in the *Device fabrication* section) needs to produce a ~ 20 mA/cm² of current density in order to refresh the channel every 1 minute. The timescale in this calculation was selected, following the repeatedly observed pumping frequency during experiment. Qualitatively speaking, the production of a higher current will generate CO₂ bubbles faster, resulting in more frequent channel refreshments and a faster flow rate of the fuel. Depending on the current density, which we control through the external electric load connecting the fuel cell electrodes, the time

for one pumping cycle varied from a few tens of seconds to minutes. The frequency of bubble pumping was measured increasing linearly with the current density, as shown in Fig. 2-6(a). The experimental result of bubble pumping is approximately half of the ideal calculated case (e.g., $\sim 40 \text{ mA/cm}^2$ required for bubble pumping frequency of 1/min). The discrepancy comes from the small bubbles near the venting area, which escape directly through the hydrophobic membrane without contributing to pump and the occasional leakage through the air-breathing cathode rather than the venting membrane. We also quantified the pumping rate by monitoring the volume of bubbles leaving the channel in Fig. 8b since the volume of bubbles is not consistent throughout the cycles. Since the diverging channel also assists refreshing the fuel, the frequency cannot give an accurate pumping rate by itself. The results show a linear trend that CO_2 production and pumping are proportional to the amount of current generated. Although the observed frequency of bubbles leaving at 50 mA/cm^2 is lower than that at 40 mA/cm^2 in Fig. 8a, the measured pumping rate at 50 mA/cm^2 is higher than that at 40 mA/cm^2 in Fig. 8b. The bubble pumping frequency is somewhat less reliable because the volumes of bubbles involved in pumping are not consistent.

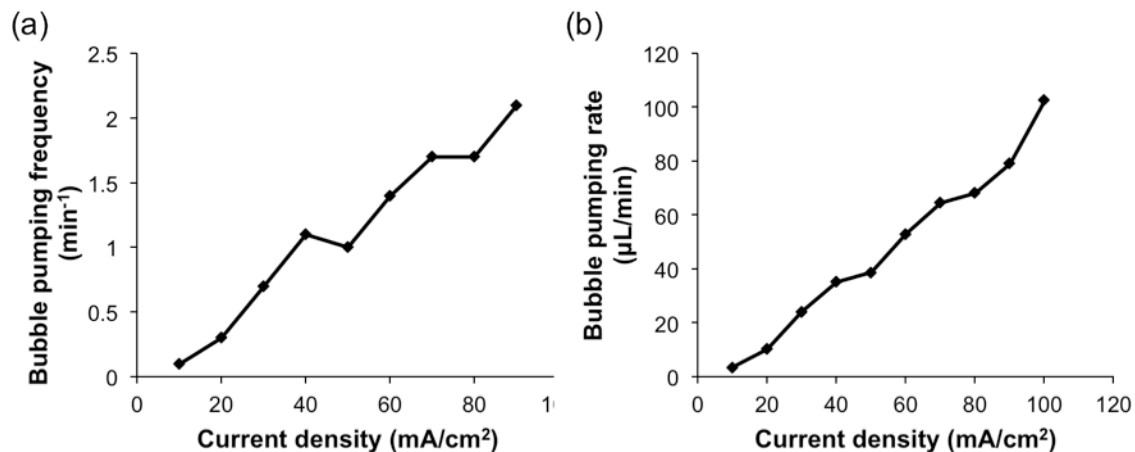


Figure 2-6: Pumping frequency and rate of designed fuel cell. (a) Frequency of bubble pumping generally increases with the current density generated. Since the frequency only counts the number of bubbles, it does not directly account for the volume of pumping. (b) Measured with the volume of each bubble leaving the venting site, the bubble pumping rate is found proportional to the current density.

In our next set of experiments, the inlet and outlet shared the same reservoir, eliminating the hydraulic pressure and recirculating the fuel. A longer testing is presented in Fig. 2-7. The device continued to refresh its channel with new streams of fuel and kept running. In contrast, once the venting site of the same device was blocked for comparison, the current density decreased soon. However, this blocked device maintained higher current densities and decreased slowly compared to Meng and Kim [30]. The discrepancy can be understood by noting some bubbles leak through the air-breathing cathode in the current device. The lost volume of bubbles is filled by the fuel from inlet or outlet, replenishing a small amount of additional fuel to the channel.

However, this supply does not have a directional pumping effect. Therefore, over time, the current eventually dies out until there is no significant bubble growth.

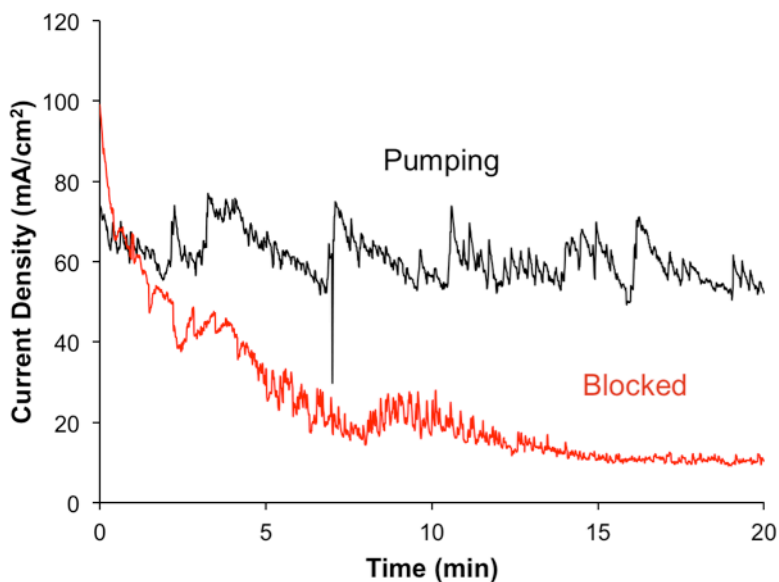


Figure 2-7: Comparison of bubble pumping enabled and blocked. During bubble pumping, a current density is maintained, and the device keeps pumping and generating power as long as fuel is available. However, when the venting site is blocked so that the bubble pumping is disabled, current density soon decreased. The experiment was done with fuel inlet and outlet connected to a common reservoir to avoid the hydraulic pressure build up. A mixture of 20 mL of 1 M fuel and 1 M electrolyte was used.

2.5.2 Air-breathing Cathode

The cathode can evaporate the excessive water formed within the cathode layer but keeps the bulk liquid inside the cell. Even though we sometimes left the cell to obtain stabilized OCP over hours, meaning no current density but evaporation through the cathode, both electrodes including air-breathing cathode did not show any sign of drying

out. We saw small water droplets condensed on the bench surface near the cathode, indicating some evaporation, when running under higher current densities ($\sim 50 \text{ mA/cm}^2$). Without any leakage seen, the cathode keeps the liquid inside the cell. At high pressures (tens of kPa), the fuel can leak through the cathode [29]. However, the proposed cell is not pressurized by any auxiliary components such as liquid pump, and brings the fuel into the reaction channel only by surface tension. The Laplace pressure built up by the bubble menisci is on the order of hundreds of Pa, which is safely lower (by two orders of magnitude) than the leakage pressure.

2.5.3 Catalytic Activities

In the conventional fuel-cell configuration, Pt is considered as a desirable option for both anode and cathode. However, the mixed potential issue [20, 24] makes it an undesirable choice to simultaneously employ Pt as the catalyst for both anode and cathode in a given mixed-reactant fuel cell. Particularly, the mixed potential issue is severe at the cathode, since Pt is prone to oxidize fuel while it is supposed to reduce oxygen. As a result, a non-noble metal is commonly used as the cathode catalyst. Contrary to this common practice, as mentioned in the *Mechanism* section, we have found an interesting phenomenon that Pt can be used as a fuel-tolerant cathode catalyst in our design. If we focus on the air-breathing cathode, O_2 is directly supplied through the air-breathing cathode from ambient air to electrolyte/catalyst interface where both the fuel (HCOOH) and supporting electrolyte (H_2SO_4) exist. Considering the equilibrium constant of HCOOH ($K_a=1.8 \times 10^{-4}$) and H_2SO_4 in water ($K=2.4 \times 10^6$), the number of HCOOH molecules desiring to break and oxidize on the cathode is far less than H^+ ions

dissociated from H_2SO_4 ready to join with O_2 from ambient air by 10 orders of magnitude. Therefore, the cathode of presented mixed-reactant fuel cell seems to have fuel tolerance.

We have further tested how the bubble pumping would affect the catalytic activities on both electrodes. Fig. 2-8 indicates that the bubble growing, moving and venting do not significantly disturb the potential between the two electrodes. First, in Fig. 2-8(a), the total disturbance in the fuel cell was monitored by investigating the OCP fluctuation while injecting bubbles through a syringe manually. The greatest disturbance of ~ 30 mV was seen when the bubble was removed to induce a rapid flow of fresh fuel mixture into the channel. On the other hand, a constant current of 30 mA/cm^2 was supplied to the cell while monitoring the cathode potential (vs. Ag/AgCl), and the bubble grew similarly to the fuel-cell reaction. Similar fluctuation behavior of ~ 30 mV at most is seen in Fig. 2-8(b). This indicates that the bubble action is disturbing mostly the cathode, which is still only a negligible effect. We also noted that, when the bubble grew to take up the space inside the channel, the potential gradually rose likely because the bubble provided a clear separation between the anode and the cathode.

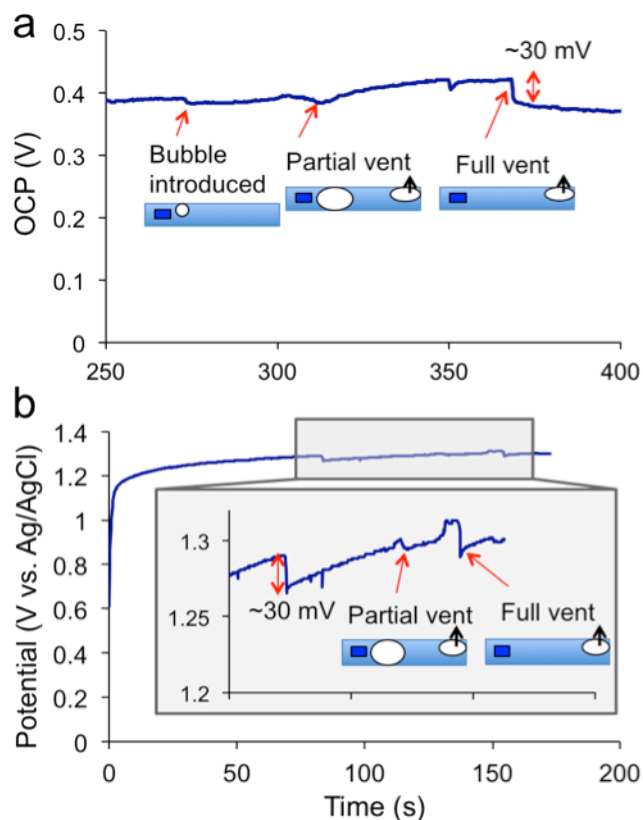


Figure 2-8: Effect of bubble pumping, moving and venting on cathode electrode. (a) The experiment was performed by manually injecting air bubbles to mimic bubble pumping while monitoring the OCP in fuel cell. The maximum observed fluctuation, which corresponded to a large bubble fully venting out and inducing a rapid stream of new fuel into the channel, was only ~ 30 mV. (b) Potential of the cathode was monitored against the reference electrode (Ag/AgCl) under a constant current of 30 mA/cm^2 to the cell. On the anode there was bubble forming and pumping similarly to the fuel-cell reaction. Potential fluctuation was ~ 30 mV, suggesting the bubble action mostly affected the cathode. Both experiments used 2 M formic acid.

Surfaces of the deposited catalysts were investigated under scanning electron microscopy (SEM). High surface area is desirable for higher electrocatalytic reaction kinetics on each electrode. Although the highly magnified view (Fig. 2-9(a)) shows a hierarchical structure in nanometer scale, the Pd black has fairly even and flat surface with little porosity in micrometer scale (Fig. 2-9(b)), which is not desirable. Compared with the electroplated version [32], the solution-deposited catalyst black used here produced less roughness in micrometer scale, which may not be sufficient to catalyze fuel-cell reactions. Electroplated catalyst black surface is expected to improve the fuel-cell performance in the next-generation devices.

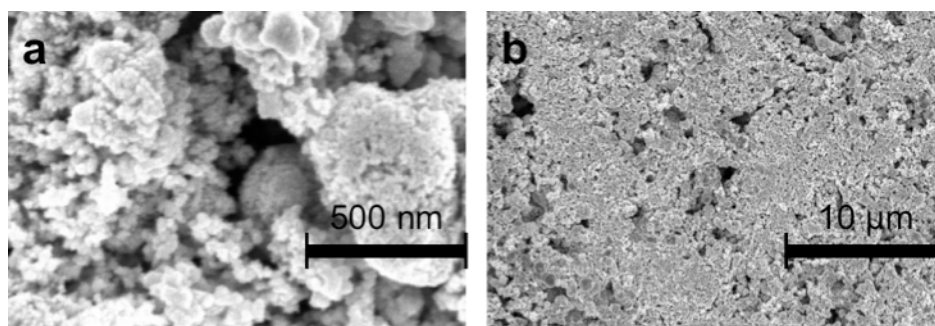


Figure 2-9: SEM images of solution-deposited Pd electrocatalyst. (a) At closer view, Pd black has cluster-like structures with nanometer scale roughness. (b) In micrometer scale view, the catalyst layer is rather flat and lacks the hierarchical structure of (a).

2.5.4 Polarization Curve

The polarization and power density curve of the fabricated devices using different HCOOH concentrations and 1 M H₂SO₄ supporting electrolyte has been tested and presented in Figs. 2-10(a) and (b). Using 1.0 M HCOOH, OCP of 0.59 V and 16.7 mW/cm² of peak power density have been obtained, and 0.5 M HCOOH also reached a

similar value of 16.1 mW/cm^2 . At higher concentration of 5 M and 10 M HCOOH, OCP dropped to 0.54 V and 0.45 V, respectively, and the current density output was decreased due to a mixing issue at the cathode. The OCP in presented device is relatively lower due to its mixed-reactant nature. Compared with other (i.e., fuel flowing by an external pump) DFAFCs utilizing quiescent air as an oxygen source, our measured value is comparable to the $\sim 12 \text{ mW/cm}^2$ of peak power density in [32], which used a silicon fabricated MEA using Pt as the cathode catalyst, and higher than the $\sim 8 \text{ mW/cm}^2$ of peak power density in [7], which used RuSeW as the fuel-tolerant cathode catalyst along with a fuel mixed with air in a vaporizer. Although the current study is to develop and prove the new concept of self-pumping fuel-cell mechanism with a mixed reactant of fuel and electrolyte, we have observed few phenomena that unveil future research directions.

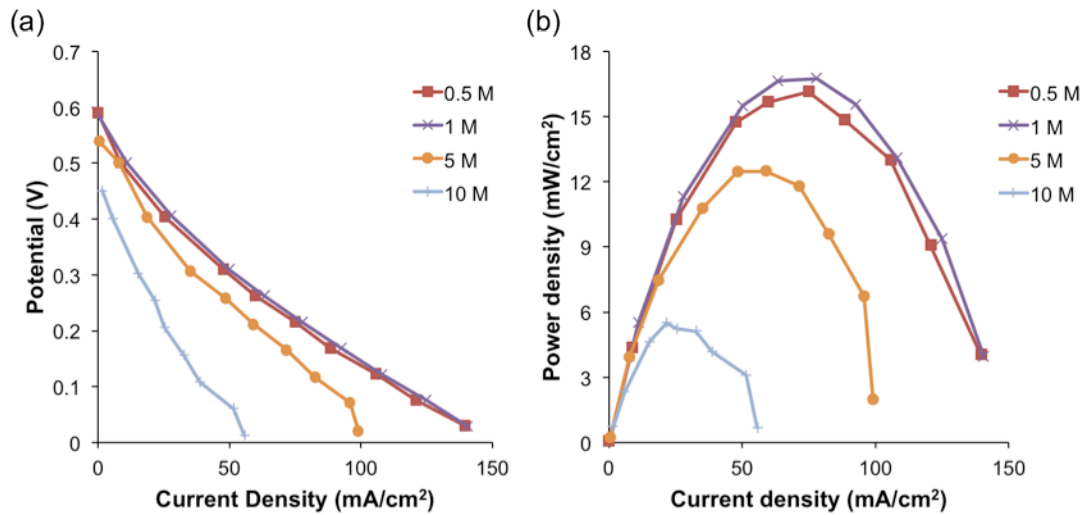


Figure 2-10: (a) Polarization and (b) power density curves of the device tested using four different HCOOH concentrations and 1 M H₂SO₄ supporting electrolyte. Polarization curve was taken under room temperature while the fuel cell was bubble pumping. At 0.5 M and 1.0 M of HCOOH, the highest peak power density was seen 16.7 mW/cm^2 , which is comparable to or higher than other DFAFCs with quiescent air as the oxygen source.

At higher concentration of 5 M and 10 M HCOOH, both OCP and current output dropped.

2.6 Conclusion

A self-standing membraneless fuel cell of a very simple design has been proposed and realized. With neither ancillary parts nor MEA, we were able to successfully build and test the fuel-cell system consisting only of a fuel-cell assembly, a fuel reservoir, and a waste reservoir. Since we have eliminated the fuel pump, oxygen tank, gas separator, and MEA, all the main issues associated with them have been cleared along with the packaging penalty. By adopting formic acid fuel in our design, the CO₂ bubbles were efficiently generated. However, the choice of fuel and oxygen supply is flexible as long as CO₂ bubbles are produced during electrochemical reaction. Using quiescent air, we have obtained the fuel-cell performance similar to or higher than other reported DFAFCs, which use an external fuel pump, under the same conditions of quiescent air. More studies are in order to understand how Pt works as a fuel-tolerant cathode catalyst in our device relative to other mixed-reactant fuel cells.

References

- [1] T. Hottinen, M. Mikkola, and P. Lund, "Evaluation of planar free-breathing polymer electrolyte membrane fuel cell design," *J. Power Sources*, vol. 129, pp. 68-72, 2004.

- [2] T. Shimizu, T. Momma, M. Mohamedi, T. Osaka, and S. Sarangapani, "Design and fabrication of pumpless small direct methanol fuel cells for portable applications," *J. Power Sources*, vol. 137, pp. 277-283, 2004.
- [3] C. Y. Chen and P. Yang, "Performance of an air-breathing direct methanol fuel cell," *J. Power Sources*, vol. 123, pp. 37-42, 2003.
- [4] S. Ha, B. Adams, and R. I. Masel, "A miniature air breathing direct formic acid fuel cell," *J. Power Sources*, vol. 128, pp. 119-124, 2004.
- [5] J. Yeom, R. S. Jayashree, C. Rastogi, M. A. Shannon, and P. J. A. Kenis, "Passive direct formic acid microfabricated fuel cells," *J. Power Sources*, vol. 160, pp. 1058-1064, 2006.
- [6] R. S. Jayashree, L. Ganes, E. R. Choban, A. Primak, D. Natarajan, L. J. Markoski, and P. J. A. Kenis, "Air-breathing laminar flow-based microfluidic fuel cell," *J. Am. Chem. Soc.*, vol. 127, pp. 16758-16759, 2005.
- [7] T. Fabian, J. D. Posener, R. O'Hayre, S.-W. Cha, J. K. Eaton, F. B. Prinz, and J. G. Santiago, "The role of ambient conditions on the performance of a planar, air-breathing hydrogen PEM fuel cell," *J. Power Sources*, vol. 161, pp. 168-182, 2006.
- [8] M. Paquin and L. G. Frechette, "Understanding cathod flooding and dry-out for water management in air breathing PEM fuel cells," *J. Power Sources*, vol. 180, pp. 440-451, 2008.
- [9] G. Q. Lu, C. Y. Wang, T. J. Yen, and X. Zhang, "Development and characterization of a silicon-based micro direct methanol fuel cell," *Electrochimica Acta*, vol. 49, pp. 821-828, 2004.

- [10] J. L. Cohen, D. J. Volpe, D. A. Westly, A. Pechenik, and H. D. Abruna, "A dual electrolyte H₂/O₂ Planar membraneless microchannel fuel cell system with open circuit potentials in excess of 1.4 V," *Langmuir*, vol. 21, pp. 3544-3550, 2005.
- [11] E. R. Choban, L. J. Markoski, A. Wieckowski, and P. J. A. Kenis, "Microfluidic fuel cell based on laminar flow," *J. Power Sources*, vol. 128, pp. 54-60, 2004.
- [12] R. Ferringo, A. D. Stroock, T. D. Clark, M. Mayer, and G. M. Whitesides, "Membraneless vanadium redox fuel cell using laminar flow," *J. Am. Chem. Soc.*, vol. 124, pp. 12930-12931, 2002.
- [13] E. Kjeang, A. G. Brolo, D. A. Harrington, N. Djilali, and D. Sinton, "Hydrogen peroxide as an oxidant for microfluidic fuel cells," *J. Electrochem. Soc.*, vol. 154, pp. B1220-B1226, 2007.
- [14] K. S. Salloum and J. D. Posner, "A membraneless microfluidic fuel cell," *J. Power Sources*, vol. 196, pp. 1229-1234, 2011.
- [15] K. S. Salloum, J. R. Hayes, C. A. Friesen, and J. D. Posner, "Sequential flow membraneless microfluidic fuel cell with porous electrodes," *J. Power Sources*, vol. 180, pp. 243-252, 2008.
- [16] E. Kjeang, R. Michel, D. A. Harrington, D. Sinton, and N. Djilali, "An alkaline microfluidic fuel cell based on formate and hypochlorite bleach," *Electrochimica Acta*, vol. 54, pp. 698-705, 2008.
- [17] T. S. Olson, B. Blizanac, B. Piela, J. R. Davey, P. Zelenay, and P. Atanassov, "Electrochemical evaluation of porous non-platinum oxygen reduction catalysts for polymer electrolyte fuel cells," *Fuel Cells*, pp. 547-553, 2009.

- [18] A. K. Shukla, R. K. Raman, and K. Scott, "Advances in mixed-reactant fuel cells," *Fuel cells*, vol. 2005, pp. 436-447, 2004.
- [19] H. Cheng, W. Yuan, and K. Scott, "A liquid-gas phase mixed-reactant fuel cell with a RuSeW cathode electrocatalyst," *J. Power Sources*, vol. 183, pp. 678-681, 2008.
- [20] D. T. Whipple, R. S. Jayashree, D. Egas, N. Alonso-Vante, and P. J. A. Kenis, "Ruthenium cluster-like chalcogenide as a methanol tolerant cathode catalyst in air-breathing laminar flow fuel cells," *Electrochimica Acta*, vol. 54, pp. 4384-4388, 2009.
- [21] K. Scott, A. K. Shukla, C. L. Jackson, Meuleman, and W. R. A, "A mixed-reactants solid-polymer electrolyte direct methanol fuel cell," *J. Power Sources*, vol. 126, pp. 67-75, 2004.
- [22] W. Sung and J.-W. Choi, "A membraneless microscale fuel cell using non-noble catalysts in alkaline solution," *J. Power Sources*, vol. 172, pp. 198-208, 2007.
- [23] E. Kjeang, N. Djilali, and D. Sinton, "Microfluidic fuel cells: A review," *J. Power Sources*, vol. 186, pp. 353-369, 2009.
- [24] J. I. Hur, D. D. Meng, and C.-J. Kim, "Membraneless micro fuel cell chip enabled by self-pumping of fuel-oxidant mixture," 23rd IEEE International Conference on Micro Electro Mechanical Systems (MEMS 2010), pp. 168-171, 2010.
- [25] D. D. Meng and C.-J. Kim, "Micropumping of liquid by directional growth and selective venting of gas bubbles," *Lab Chip*, vol. 8, pp. 958-968, 2008.
- [26] D. D. Meng and C.-J. Kim, "An active micro-direct methanol fuel cell with self-circulation of fuel and built-in removal of CO₂ bubbles," *J. Power Sources*, vol. 194, pp. 445-450, 2009.

- [27] Z. Liu, L. Hong, M. P. Tham, T. H. Lim, and H. Jiang, "Nanostructured Pt/C and Pd/C catalysts for direct formic acid fuel cells," *J. Power Sources*, vol. 161, pp. 831-835, 2006.
- [28] C. Rice, S. Ha, R. I. Masel, P. Waszczuk, A. Wieckowski, and T. Barnrad, "Direct formic acid fuel cells," *J. Power Sources*, vol. 111, pp. 83-89, 2002.
- [29] R. S. Jayashree, J. S. Spendelow, J. Yeom, C. Rastogi, M. A. Shannon, and P. J. A. Kenis, "Characterization and application of electrodeposited Pt, Pt/Pd, and Pd catalyst structures for direct formic acid micro fuel cells," *Electrochimica Acta*, vol. 50, pp. 4674-4682, 2005.
- [30] D. D. Meng and C.-J. Kim, "An active micro-direct methanol fuel cell with self-circulation of fuel and built-in removal of CO₂ bubbles," *J. Power Sources*, vol. 194, pp. 445-450, 2009.
- [31] J. I. Hur, D. D. Meng, and C.-J. Kim, "Membraneless micro fuel cell chip enabled by self-pumping of fuel-oxidant mixture," 23rd IEEE International Conference on Micro Electro Mechanical Systems (MEMS 2010), pp. 168-171, 2010.
- [32] J. Yeom, R. S. Jayashree, C. Rastogi, M. A. Shannon, and P. J. A. Kenis, "Passive direct formic acid microfabricated fuel cells," *J. Power Sources*, vol. 160, pp. 1058-1064, 2006.

CHAPTER 3

MINIATURIZATION OF THE AIR-BREATHING FUEL CELL

For our continuous effort to realize portable miniature fuel cells in various scales, the next step was to design a scaled-down version of the fuel cell developed in Chapter 2, which was in a dimension comparable to a AA battery or even a cell phone battery. Here we introduce our new miniature fuel cell with overall dimensions in few millimeter scales, adequate for integration with MEMS devices and comparable to the smallest button batteries.

3.1 Overall design

Further miniaturized fuel cell was designed by utilizing photolithographic micromachining techniques common to MEMS. Micromachining was chosen since traditional machining is limited and difficult to handle. Dimensions are shrunk to approximately 1/10 of the previously reported prototype, i.e., from centimeters to millimeters. Channel of the fuel cell being 1 mm wide, 3 mm long, and 500 μm thick, the overall packaging of the miniaturized fuel cell in this chapter is 4 mm x 7 mm x 2 mm without the fuel cartridge. Although the developed fuel cell is well shrunk in size, the miniaturization is not hindered by packaging penalty in this case, since the check valve and the CO₂ breather, the components required for self-circulation of the fuel can be designed into any shape without occupying bulky space in the micro fuel cell.

The inlet, outlet, and breather is defined on anode and processed through silicon microfabrication. Since it is challenging to assemble a nanoporous hydrophobic membrane as a CO₂ breather into this ultra-compact fuel cell, we embedded the breather into the anode part with small through holes on silicon anode with local hydrophobic drop coating with Cytop[®]. Further deposition of Cr/Au current collector layer and Pd catalyst deposition is performed on anode chips for the anodic reaction.

The channel structure with check valve is defined in silicon wafer and etched through. Thermal oxidation ensures the hydrophilicity of the channel to the fuel and electrolyte mixture for spontaneous wetting of the fuel inside the channel. The fabricated parts are assembled by sandwiching the channel structure between the fabricated anode and gas diffusion electrode cut into the size of fuel cell.

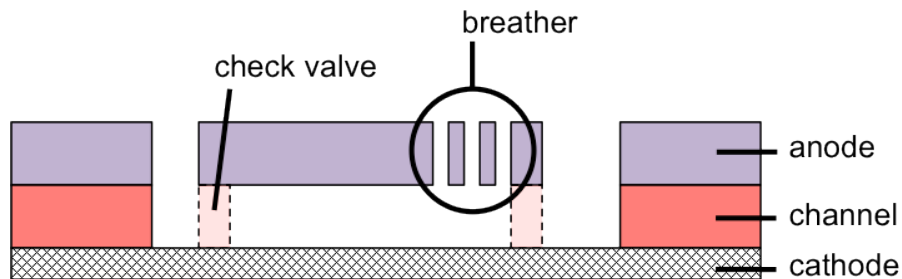


Figure 3-1: Further miniaturized fuel cell with microfabricated anode and channel. Check valve and breather, the components needed for bubble pumping, are all miniaturized and embedded in the micro fuel cell design developed in this chapter.

In order to keep the electrical passivation between the two electrodes, each component was thermally oxidized before the assembly. Moreover for easier connection from outside, channel was designed narrower in the width so that the electrical connection from anode and cathode could be reached through the exposed gap.

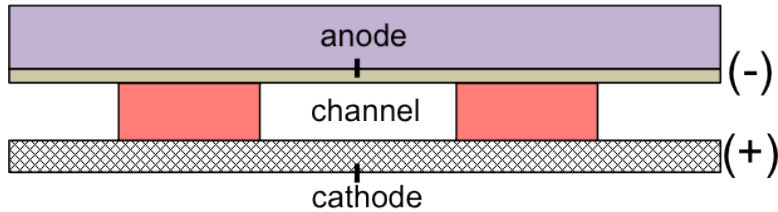


Figure 3-2: Another side view of the micro fuel cell. Electrical connection of the fuel cell faces inner surface for electrochemical reaction in the channel side. The channel is narrower than anode and cathode so that electrical connection from the outside can easily reach in between the gap.

The top view of the overlaid anode and channel plate in Fig. 3-3 shows the shape of the channel and designed check valve, and where the wire comes in for anodic connection. Any wire thinner than 500 μm will fit in between the gap and be placed securely with an adhesive tape that provides electrical passivation between anode and cathode.

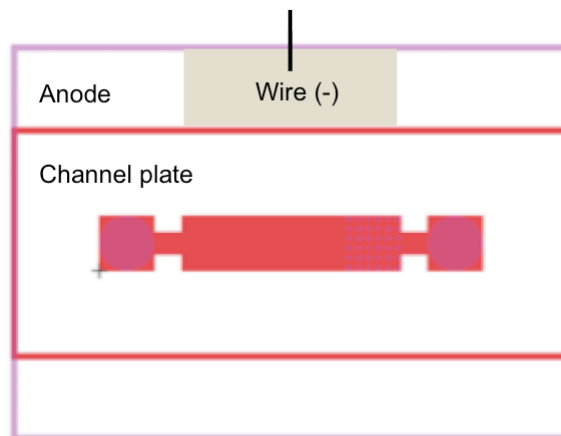


Figure 3-3: Top view of the overlaid channel plate and anode. Any wire thinner than 500 μm should fit in the gap.

3.2 Fabrication

Anode and channel was designed to fit in one 4" wafer, using single mask. The through-etching process defined the structures of anode and channel and also released each chips. The whole process flow is described in Fig. 3-4. On a test silicon wafer, 3 μm of silicon dioxide layer is deposited using PECVD. The deposited oxide serves as DRIE mask during the through hole etching. In order to define the DRIE mask, the deposited oxide is patterned using photolithography with AZ 5214 photoresist. After using AOE process to define oxide mask, DRIE was performed to etch through the wafer. Subsequently, thorough cleaning was performed with ALEG, Piranha and BOE before the samples were put into thermal oxidation chamber.

Anode chip still needs a current collector and anodic electrocatalyst layer for fuel oxidation. After the oxidation, anode is deposited with evaporated Cr/Au with corresponding thickness of 20/200 nm using shadow mask. A Pd layer was drop

deposited using same method and loading used in Chapter 2. Appropriate volume for the given area is measured out to result in 2 mg/cm² of Pd using pipette, and the catalyst ink stayed within the defined region of evaporated Au layer.

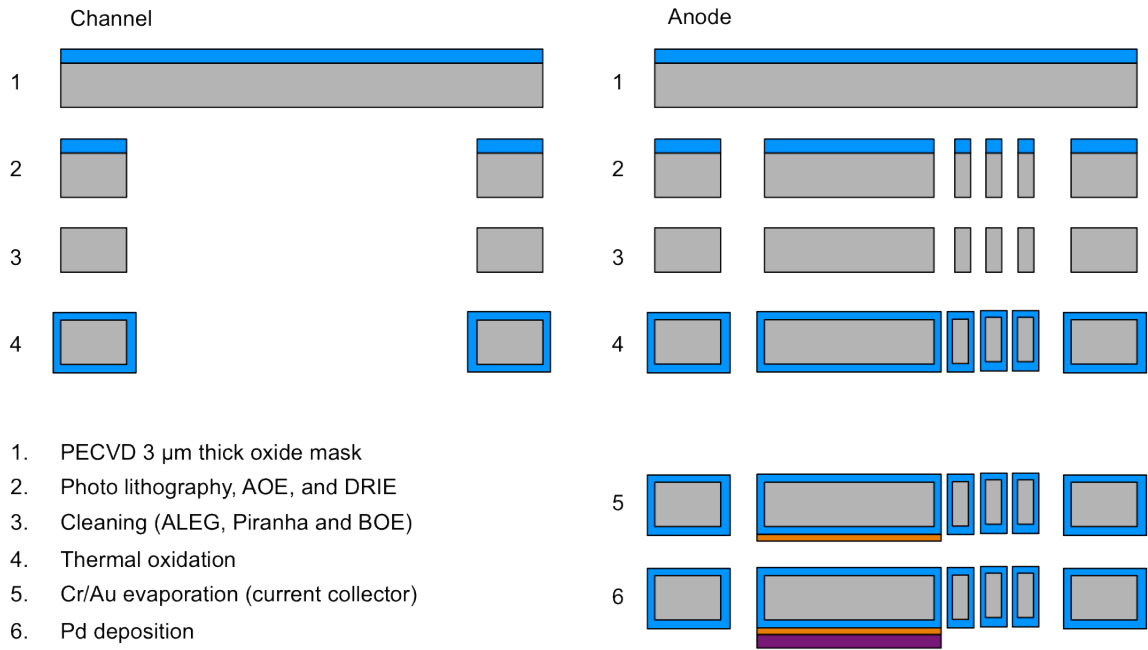


Figure 3-4: Fabrication process flow for micro fuel cells. Channel and anode chips were processed together on a 4” silicon wafer using single mask until the anode needs subsequent current collector and anodic electrocatalyst deposition.

Fabricated parts of channels and anodes with different channel lengths are shown in Figure 3-5. After the DRIE release of the channels and anodes with etched through structures, anode went through Cr/Au evaporation with shadow mask as shown in the figure.

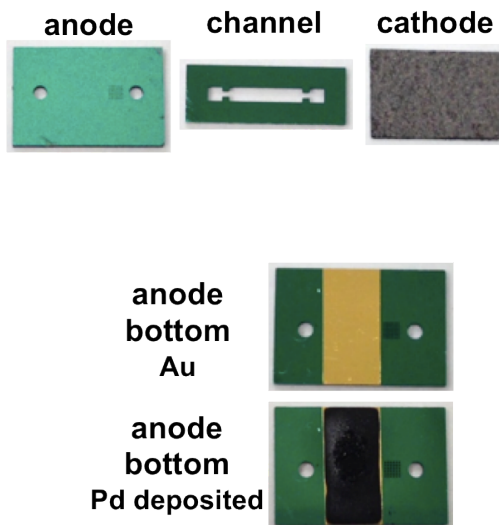


Figure 3-5: Photographs taken during fabrication of fuel cell components: anode, channel and cathode.

After all the parts are fabricated, cathode is prepared by cutting GDE into 4 mm x 7 mm to match the size of anode. Since the carbon paper is rather floppy and weak, another channel was used as a support material on the bottom of cathode for easy clamping without damaging the material. Copper tape is attached to the anode current collector on the bottom side of anode for extension of the electrode and easy access from the outside.

As shown in the Figure 3-6, the assembled final micro fuel cell is smaller than the size of one's thumbnail and no significant leakage of fuel has been observed. Both electrodes, anode and cathode were connected to the potentiostat with alligator clips during the testing.

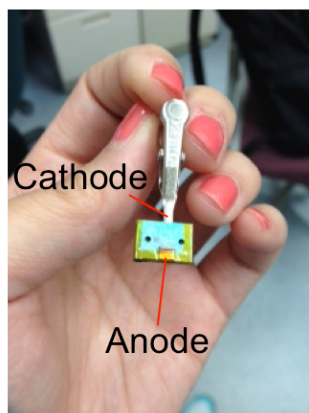


Figure 3-6: Micro fuel cell assembled into packaging smaller than a thumbnail.

3.3 Catalyst support (Graphite vs. Cr/Au)

Due to the change in catalyst support material from graphite (Chapter 2) to evaporated Cr/Au on oxidized silicon wafer (this chapter), we studied the fuel oxidation pattern on each catalyst support to confirm that the electrocatalytic fuel cell reaction will not be greatly modified due to the change.

The key requirements for catalyst support are (1) high specific surface area, (2) high electrochemical stability under fuel cell environment and (3) high electrical conductivity. Most commonly used as catalyst support is Vulcan XC-72 carbon black, which commercial MEAs are based on [1, 2]. However, in our case of silicon wafer, we need to deposit our own catalyst support that can also serve as current collector.

Our choice was to evaporate Cr/Au layer on the substrate. Since the catalyst support layer plays role in electrochemical behavior in fuel oxidation and oxygen reduction, we needed to study the effect of the change in catalyst support layer. To compare and test the effect of having Cr/Au catalyst support, Pd catalyst was both

deposited with same loading, 2 mg/cm^2 , on graphite plate and oxidized silicon substrate with Cr/Au current collector. After proper drying and baking at $120 \text{ }^\circ\text{C}$, two electrodes were tested in a beaker to observe the half-cell behavior.

Result was promising that the rate of fuel oxidization has not degraded after changing the catalyst support from graphite to evaporated gold (Fig. 3-7). The gold support/current collector seemed to even improve the electrocatalytic activity in fuel/electrolyte mixture and show comparable or higher current density at given potential. Thus we concluded that our design with evaporated Cr/Au layer is feasible and acceptable.

Now that the catalyst for anode is confirmed to behave similarly to the fuel cell developed in Chapter 2, the miniaturized fuel cell components in this chapter can be characterized and compared with their larger counterparts in Chapter 2.

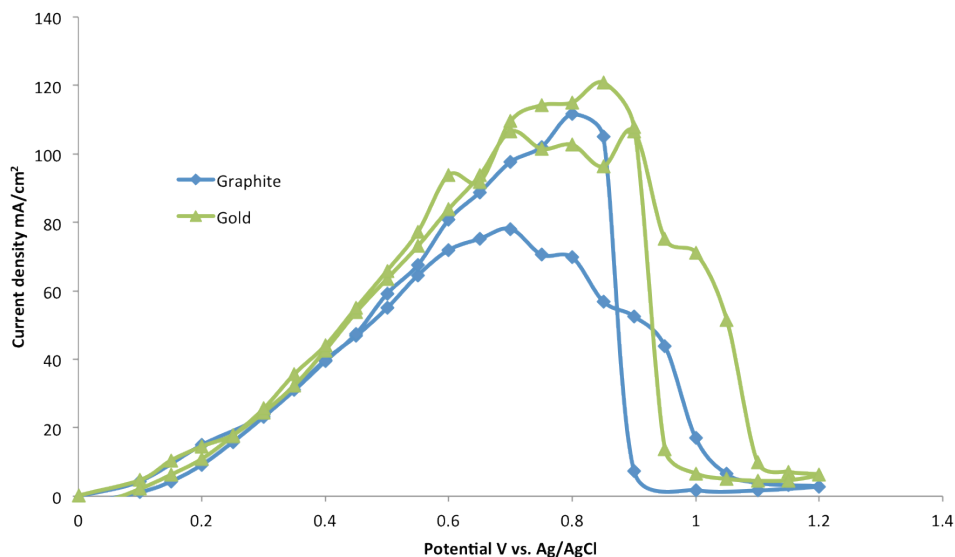


Figure 3-7: Half-cell tests of graphite and Cr/Au catalyst support layers in 1 M fuel (HCOOH) in electrolyte (1 M H_2SO_4 in DI water).

3.4 Resulting output of the developed micro fuel cell

Assembled device was tested using Keithley 2400 series controlled with Labview to record the data. Normalized with the electrode area, 0.03 cm^2 , at maximum while pumping the miniature fuel cell outputted 163 mA/cm^2 . The miniature fuel cell is expected to show a behavior similar to the 10 times larger system of the previous chapter since the catalyst material is the same and the concentrations of the fuel/electrolyte mixture is the same. However, the maximum current output seemed to be higher than what we have seen normally, i.e., $\sim 120 \text{ mA/cm}^2$ at maximum. A possible reason for the higher current density can be some leakage of fuel through the seal between the channel and anode plate, resulting in slightly larger active catalyst surface than the defined area. Another possible explanation can be that, as seen in Figure 3-7, the fuel oxidation on Cr/Au was slightly higher than just graphite and there might be a minor improvement in fuel oxidation when having Cr/Au catalyst support.

OCP of the assembled miniature fuel cell was also found to be 0.55 V , a value similar to the larger scale counterpart of current fuel cell design. This indicates that although the fuel cell is shrunk by an order of magnitude, the chemistry between the two electrodes is kept the same and the fuel crossover or other issues are not any more severe.

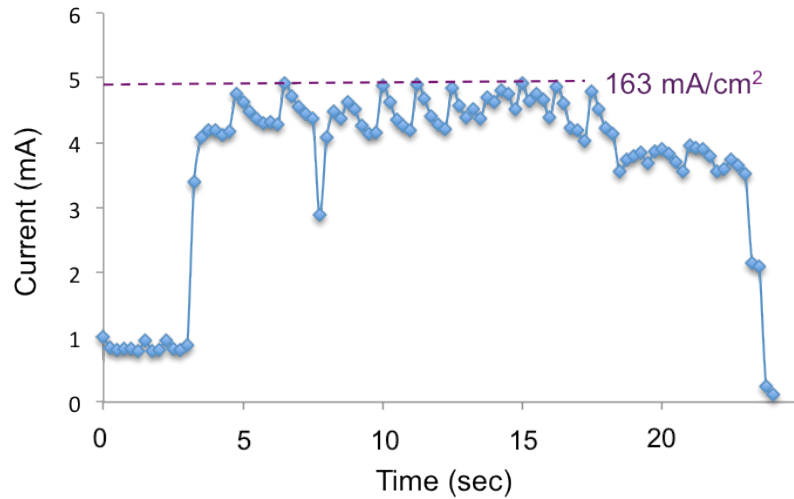


Figure 3-8: Maximum current density output was 163 mA/cm^2 while fuel cell circuit was closed with 0 V between the two electrodes (shorted).

The pumping effect inside the channel is no longer visible through the fuel cell structure since all the components are of silicon and not transparent. The only way to observe the pumping is monitoring the current density fluctuation along time. Indication of bubble fill up and venting is a gradual current decrease and sudden surge of current, respectively. The phenomenon is witnessed in the previous prototype where we could observe the bubble behavior and current density at the same time through the side of the transparent channel plate. At reduced current density, pumping effect was observed at reduced current density, 67 mA/cm^2 . The time for CO_2 to fill up the channel volume at the given average current density is 8 seconds, which match the current fluctuation pattern along time.

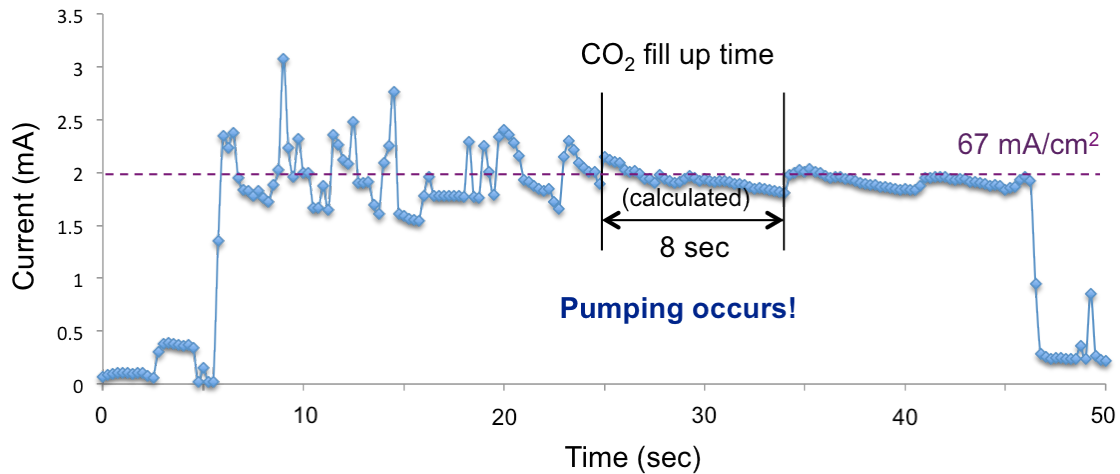


Figure 3-9: Pumping effect was observed at reduced current density, 67 mA/cm^2 . The time for CO_2 to fill up the channel volume at the given average current density is 8 seconds, which match the current fluctuation pattern along time.

The miniature fuel cell has been successfully built based on silicon microfabrication technique and was verified to perform comparable to or better than the one order of magnitude larger prototype of the previous chapter. The pumping effect was also indirectly observed. Although careful design and fabrication technique will further be required to advance this smaller-than-thumbnail size fuel cells to the level of good performance, this chapter proved the concept of shrinking the entire system within $\sim 0.05 \text{ cm}^3$ of volume without encountering the “packaging penalty”.

Reference

- [1] Y. Shao, J. Liu, Y. Wang, and Y. Lin, “Novel catalyst support materials for PEM fuel cells: current status and future prospects,” *J. of Materials Chemistry*, vol. 19, pp. 46-59, 2009.

- [2] Y. Zhou, K. Neyerlin, T. S. Olson, S. Pylypenko, J. Bult, H. N. Dinh, T. Gennett, Z. Shao and R. O'Hayre, "Enhancement of Pt and Pt-alloy fuel cell catalyst activity and durability via nitrogen-modified carbon supports," *Energy Environ. Sci.*, vol. 3, pp. 1437-1446, 2010.

CHAPTER 4

OXYGEN GENERATING AND LIMITING CATHODE

4.1 Introduction

In Chapter 2, we have eliminated the problematic MEA and bulky oxygen tank from fuel cell system so that the resultant fuel cell is composed of only active channel and electrode component and fuel reservoir. The fuel cell is free of “packaging penalty” and miniaturizable in any dimension as far as it is manufacturable. However, the oxygen supply method is restricted to the availability of ample air from environment, which would not allow stacking of multiple fuel cells for higher power and energy capacity. We need to solve the problem of oxygen supply to the cathodic chamber in order to realize a miniature fuel cell that allows stacking.

Most of the microfluidic fuel cells bear mass-transport-rate-limited process on the cathodic site, which predominantly limits the current density of those fuel cells. The fuel cells based on dissolved oxygen were particularly limited by the low solubility of oxygen. Jayashree et al. [1] incorporated a gas diffusion electrode as an air-breathing cathode that allowed gaseous oxygen transport from the ambient air. The oxygen available from ambient air has advantages over the oxygen dissolved in aqueous media due to its higher diffusivity and concentration. After further development, power density as high as 70 mW/cm^2 was achieved with DMFCs based on air-breathing LFFC [2]. However, air-breathing designs need a constantly pumped stream of electrolyte on cathode to prevent the fuel from crossing over and conducting ions through between the electrodes. They are

also inherently dependent on the free convection of oxygen from ambient air to the cathode. Therefore, the system will lose its flexibility in choosing operating environments, and scaled-up applications, where most likely the miniature fuel cells will need to be stacked on top of each other (Fig. 4-1), will face difficulties.

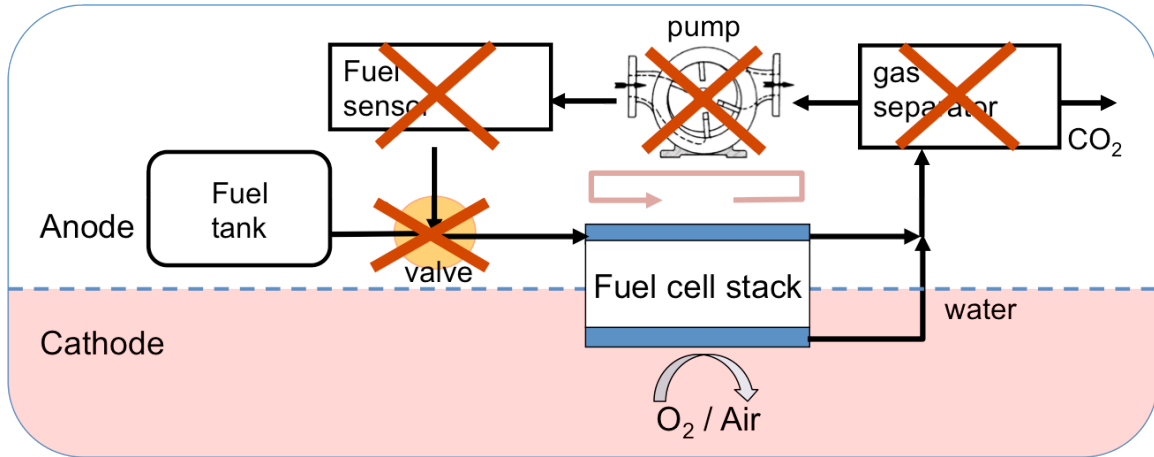


Figure 4-1: Schematic illustration of components needed in conventional microfluidic fuel cells and the eliminated components in our previous micro fuel cells. Oxygen supply in cathodic half-cell is the only component requiring improvement in realizing stackable miniature fuel cells.

The performance of microfluidic fuel cells can be improved by employing aqueous oxidants that are soluble at higher concentrations than dissolved oxygen. For example, power densities up to 38 mW/cm² and 70 mW/cm² have been obtained using vanadium redox couples as both fuel and oxidant [3]. These redox fuel cells benefit from balanced anodic and cathodic streams. Similarly, a microfluidic fuel cell was demonstrated employing hydrogen peroxide as both fuel and oxidant [4]. The operation of that cell, however, was dependent on a net consumption of supporting electrolyte, with

23 mW/cm² at most when 0.75 M hydrogen peroxide was used. A DMFC based on MEA has been tested using 3% hydrogen peroxide solution. At room temperature, a power density of 16 mW/cm² was available and 24 mW/cm² was achieved when operated at 42 °C. Also, Kjeang et al. [5] have reported a membraneless microfluidic fuel cell, using 1-3 M hydrogen peroxide as a cathodic stream. A high power density of ~30 mW/cm² was drawn from this fuel cell, which was comparable to an air-breathing fuel cell using formic acid (26 mW/cm²) and better than fuel cells based on dissolved oxygen (0.2 mW/cm²). However, the microfluidic fuel cells still needed a vigorous fuel and oxidant delivery method (i.e., external liquid pumps) to prevent the bubble clogging and fuel crossover; otherwise, MEA should be used.

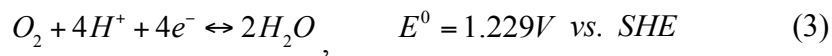
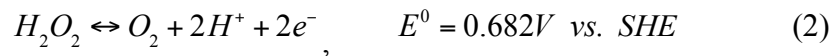
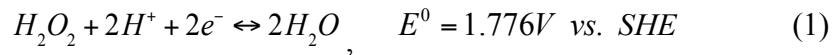
To obtain a fuel cell of solid-state construction complete with self-regulated deliveries of both fuel and oxygen, we propose a new microfluidic fuel-cell design that uses hydrogen peroxide as the oxidant in conjunction with the self-pumping fuel. Like common liquid fuels (e.g., methanol, formic acid), hydrogen peroxide is readily supplied at high concentrations and can be dissolved in aqueous media, balancing the overall reaction rate in the cell. The fuel-cell performance will no longer be limited by the cathodic reaction or dependent on the environment around the fuel cell. Since a cathode does not need to breath air, the unit fuel cells can be stacked for higher power output. Standalone with no moving part and no interconnect, the solid-state construction makes the resulting fuel-cell system truly scalable.

To combat the “packaging penalty,” we have been striving to systematically eliminate all of the fuel cell’s ancillary components. An ideal design would be a microfluidic fuel cell that operates in a self-regulated fashion with no moving parts. So

far, we have eliminated the need for fuel pumps and gas separators using a bubble pumping mechanism [6]. While simplifying the design of the fuel cell [7, 8], the air-breathing cathode required ample air convection. This need, unfortunately, makes it difficult to design fuel cells that can be stacked into a large system in the future.

In order to overcome the problem of oxidant being the limiting factor in the fuel cell, a number of researchers have sought alternative oxygen sources. Ideally, these alternatives should actively supply oxygen into a constrained environment, where ambient air is not available, with concentration higher than that of the dissolved oxygen in the liquid stream [3, 9]. Employing hydrogen peroxide as an oxidant for microfluidic fuel cells has been considered promising and attractive [4, 5, 10] due to its fast decomposition and easy storage in a liquid state.

Adopting hydrogen peroxide into a microfluidic fuel cell is attractive for solving the oxygen deficiency issue. Hydrogen peroxide inherently has a high standard reduction potential as shown in Equation 1. However, equation 2 readily occurs on electrodes resulting in a mixed potential at 0.85 V. Instead, generated oxygen can be reduced into water through reaction 3. If the decomposed oxygen from hydrogen peroxide is harvested and used properly in the cathode, the waste is reduced.



However, rigorous oxygen generation on the catalyst surface wastes hydrogen peroxide during non-operation, and the cathode channel is subject to severe dry-out if hydrogen peroxide is not removed (pumped out). Here, we designed a self-regulated oxygen generating cathode integrated in a monolithically fabricated electrode without any need for ancillary parts (e.g., pumps).

4.2 Mechanism

Figure 4-2 illustrates the working mechanism of the proposed cathode. In the current report, a catalyst is coated only inside the micro-pockets formed on the surface of the container. When bulk solution of catholyte containing hydrogen peroxide initially comes into contact with Pt black deposited inside the micro-pockets, hydrogen peroxide instantly and readily decomposes into oxygen gas and fills each pocket. Once the oxygen bubble fully occupies the pocket, the presence of the bubble separates the bulk liquid containing hydrogen peroxide from the Pt, preventing any further reaction, and the bubble ceases to grow. During fuel-cell operation some of the oxygen is reduced to water, so that the bubble starts to shrink. As such, some of the catalyst is once again exposed to the bulk liquid, producing oxygen anew and growing the bubble again. Aside from the hydrogen peroxide that is directly reduced to water, the size of the oxygen bubble is self-regulated and the oxygen bubbles are always ready to be reduced to water when in demand.

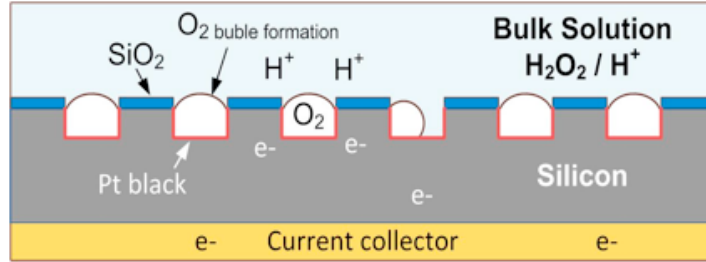


Figure 4-2: Schematic drawing of microstructured cathode. When bulk solution of catholyte containing H_2O_2 contacts Pt black deposited inside the micro-pockets, O_2 bubbles instantly grow to fill up the structure. Further O_2 bubble growth is blocked by the bubble itself, which separates Pt from bulk solution. During fuel-cell operation, O_2 is consumed so the bubbles shrink, allowing the bulk solution to contact the Pt causing the O_2 bubbles to grow again.

4.3 Fabrication

Our self-regulated cathode has been developed by microfabricating the structures in a monolithic manner. We started fabrication on a highly doped silicon wafer ($0.0015 \Omega \cdot \text{cm}$) so that the collection of current generated from the fuel-cell reaction can be directly drawn through the backside of the silicon. A thick photoresist (PR), AZ 4620, is used to both pattern deposited silicon dioxide and to etch the exposed silicon using deep reactive ion etching (DRIE) (Figs. 4-3(a) & (b)), forming an array of holes $100 \mu\text{m}$ in diameter and $50 \mu\text{m}$ deep. After the DRIE process, the polymer deposited inside the structures was removed by 1 min of oxygen plasma etching. A conformal gold seed layer is deposited using a planetary carousel in an e-beam evaporator to cover both sidewall and bottom surfaces inside the microstructures (Fig. 4-3(c)), followed by a lift-off process

to expose the oxide passivation (Fig. 4-3(d)). The thick PR has furthermore served as a lift-off resist after evaporation of gold. Pt black is plated onto the gold surface inside each hole using 1.0%w/w chloroplatinic acid and 6.0%w/w ammonium phosphate (Fig. 4-3(e)). Loading of 2 mg/cm² was targeted at -0.5 V vs. Ag/AgCl using a potentiostat (Princeton Applied Research 263A). Prior to electroplating the catalyst, we first wet the micro-pockets with methanol to make sure the plating solution is in contact with the seed layer and Pt plating is uniform throughout the sample.

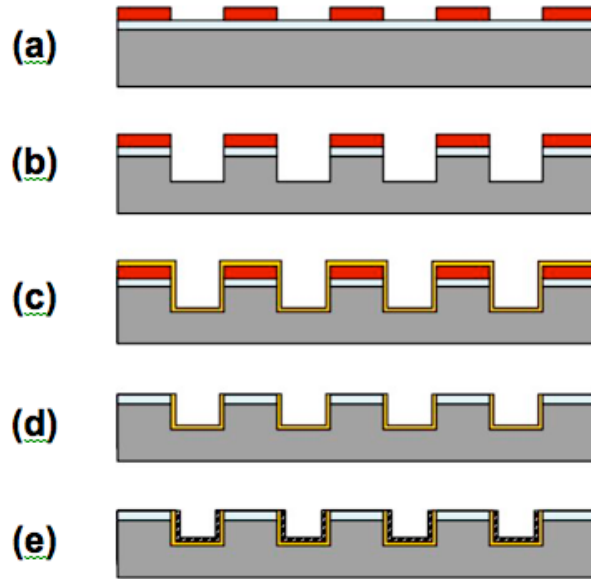


Figure 4-3: Fabrication of the device. (a) Photoresist is deposited and patterned on top of oxide-coated Si wafer, (b) silicon is etched by DRIE, (c) gold is evaporated to form a seed layer, (d) gold is selectively removed by lift-off, and (e) Pt black is plated on the gold surface.

The fabricated device is 3 mm × 3 mm, and the active catalyst deposited surface area including the sidewall and bottom is 0.078 cm² (Fig. 4-4(a)). A close view of the structures by scanning electron microscopy (SEM) shows selective deposition of catalyst

inside the structures and as well as the silicon dioxide passivation layer to prevent oxygen formation outside of micro-pockets. SEM figures confirm successful deposition of 500 nm Pt black on both the scalloped (from DRIE) sidewall and bottom surface (Fig. 4-4(c)).

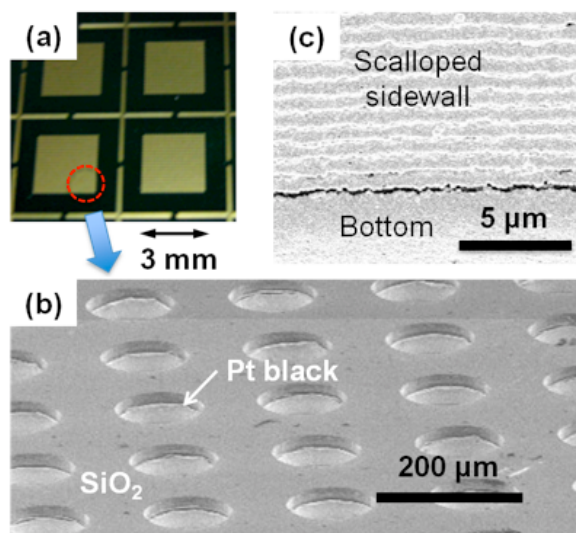


Figure 4-4: (a) Fabricated device, (b) SEM image of the cathode shows conformally deposited Pt black, and (c) image of scalloped DRIE sidewall and bottom surfaces.

4.4 Experiment

The electrochemical half-cell behavior of the fabricated cathode has been evaluated using cyclic voltammetry and potentiostatic measurements in a three-electrode electrochemical cell. The catholyte consisted of an electrolyte of 1 M H₂SO₄ (sulfuric acid) for proton conduction and 0.1 M H₂O₂ as an oxidant. First, cyclic voltammetry was performed in a blank electrolyte without oxidant to compare the effect of hydrogen peroxide in oxygen reduction in the half-cell test. In addition, to simulate a mixed-reactant condition, 1 M HCOOH (formic acid) is added to the catholyte.

Bubble formation was observed under the microscope over time. While the structured cathode is immersed in the catholyte, video was taken focused at the pit. A color difference is observed when the bubble grows in volume, from the top. Bubbles were also observed using a 3D camera (HiROX) from different angles in order to confirm whether the bubble is well contained inside the structure and discern the location of the bubble meniscus on the structure.

The electrocatalytic activity of the structured Pt toward hydrogen peroxide reduction was analyzed by obtaining polarization data for cathode performance evaluation. A polarization curve for the Pd anode was also obtained from separate half-cell tests. The anode used here was prepared by solution depositing Pd ink on a graphite plate to obtain catalyst loading of 2 mg/cm^2 and Nafion loading of 0.1 mg/cm^2 . The anolyte used here is 1 M HCOOH in 1 M H₂SO₄ in deionized water. Obtained data is normalized to the surface area.

4.5 Results and discussion

4.5.1 Electrochemical Activity

Electrochemical properties of the fabricated cathode are assessed using cyclic voltammetry as shown in Fig. 4-5. Sweeping in a blank solution of electrolyte alone shows a cyclic voltammetry pattern that is distinctive to a Pt electrode in contact with aqueous H₂SO₄. Upon addition of H₂O₂ into the solution, the open circuit potential (OCP) increases to 0.6 V vs. Ag/AgCl and starts showing reduction current below 0.5 V. A similar trend is maintained after HCOOH is added to simulate a fuel crossover, although it is slightly shifted to the positive side, implying some fuel is being oxidized

and giving mixed potential. However, even in a mixed-reactant condition the fabricated electrode can still maintain its ability to give reduction current to function as a cathode.

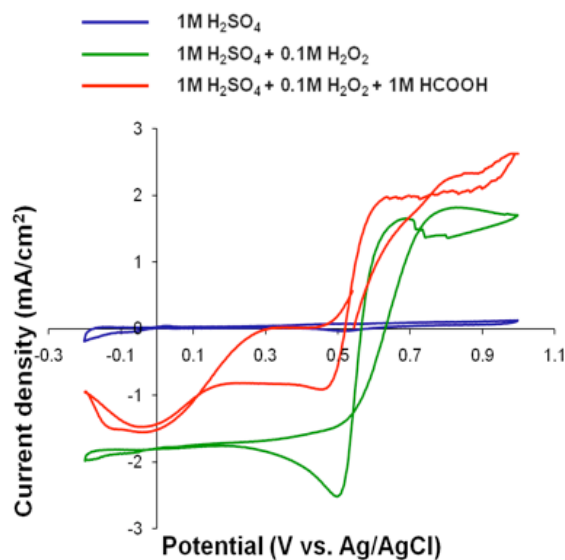


Figure 4-5: Cyclic voltammetry of fabricated cathode. The reported device shows reduction current under 0.55 V when H₂O₂ is added. Even after adding HCOOH, although the current is decreased, it still functions as a cathode.

4.5.2 Self-Regulation of O₂ Bubbles

In another experiment to investigate the behavior of bubbles, the cathode is exposed to a bulk solution of 1 M H₂SO₄ containing 0.1 M H₂O₂. The pockets were instantly filled with oxygen supply from hydrogen peroxide decomposition on contact with the catalyst. We found the bubble formation is selective and only forms inside the pockets and not on the silicon dioxide passivation surface. The cathode micro-pockets successfully contained the oxygen bubbles for over 2 hours, blocking further decomposition of hydrogen peroxide while not under fuel-cell operation (Fig. 4-6). Although the change in the color and imaging view from the side indicates bubble growth

in volume, the generation rate is not rigorous enough to let the oxygen bubble leave the structure, therefore the generated oxygen is not wasted down the stream, a problem from which other H_2O_2 -utilizing microfluidic fuel cells suffer. Furthermore, oxygen bubble growth indicates that the catalyst and bulk solution are not completely separated from each other, so that when in fuel-cell operation mode protons from the bulk can conduct to the catalyst to some extent to complete the oxygen reduction.

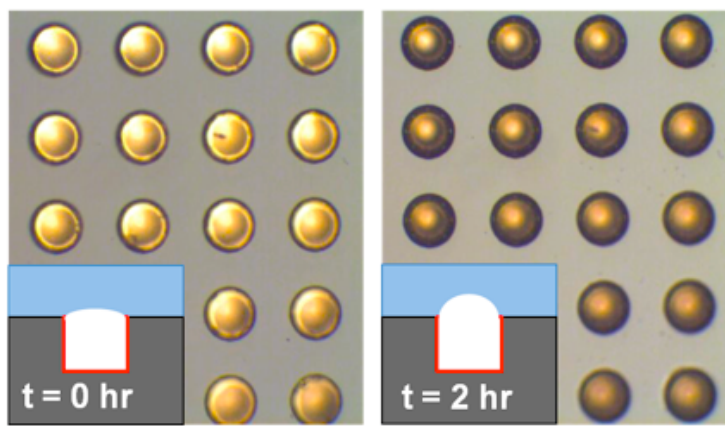


Figure 4-6: Oxygen bubbles form inside the micro-pockets selectively. Even after 2 hours, oxygen bubbles, which grew in volume, are well contained in the structures.

We have also confirmed that the generated oxygen bubbles are consumed during fuel-cell operation. Under potentiostatic half-cell operation of the cathode, applying 0 – 0.3 V vs. Ag/AgCl resulted in a reduction in bubble size, showing that the cathode makes use of the naturally decomposed oxygen bubbles. As soon as the circuit is open, i.e., the load is removed, micro-pockets are instantly refilled with oxygen bubbles and further decomposition of oxygen and waste is prevented in a self-regulated manner.

4.5.3 Polarization Curve

Half-cell tests of anode (Pd-deposited on graphite in 1 M HCOOH in 1 M H₂SO₄) and cathode show reasonable current outputs (Fig. 4-7), suggesting that they can indeed function as a fuel cell when combined into one device. The OCP of the proposed full fuel cell is ~1 V with no need for oxygen supply from a pressurized tank or ambient air. The normalized current density suggests that the cathode and oxygen supply is not a limiting factor any more. With the concept proven and the device characterized, we are optimizing the structure dimensions for higher hydrogen peroxide concentrations.

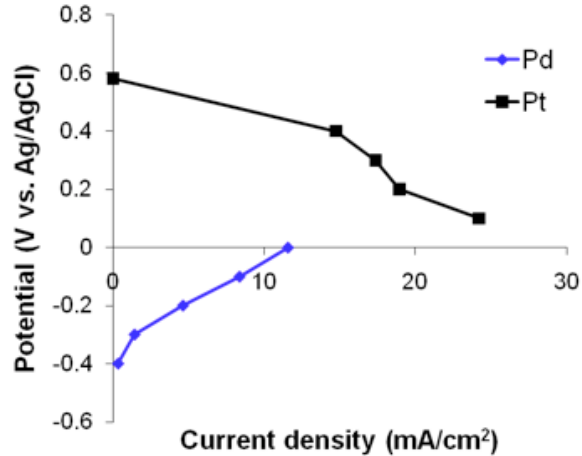


Figure 4-7: Half-cell tested cathode and anode show promising results with OCP of 1 V and current density output comparable to existing micro fuel cells.

4.6 Conclusion

We have proposed and developed a monolithically microstructured cathode that self-regulates the generation and consumption of fuel cell oxygen supply. In the context of eliminating ancillary components to realize a truly miniaturized fuel cell, the cathode reported here successfully controls the oxygen supply only when in need without any

help from other components. Electrochemical testing and visual observation together confirmed the working mechanism of the cathode as designed. Upon improvement and optimization of this proof-of-concept cathode and its integration into a full fuel cell, a reasonable power output is expected. When successfully implemented, fuel cell performance will no longer be a cathode-limited reaction, nor depend on the environment around the fuel cell. Since the cathode does not need to breathe air, stacking of multiple unit fuel cells will become feasible for higher power output.

References

- [1] R. S. Jayashree, L. Ganes, E. R. Choban, A. Primak, D. Natarajan, L. J. Markoski, and P. J. A. Kenis, "Air-breathing laminar flow-based microfluidic fuel cell," *J. Am. Chem. Soc.*, vol. 127, pp. 16758-16759, 2005.
- [2] A. S. Hollinger, R. J. Maloney, R. S. Jayashree, D. Natarajan, L. J. Markoski, and P. J. A. Kenis, "Nanoporous separator and low fuel concentration to minimize crossover in direct methanol laminar flow fuel cells," *J. Power Sources*, vol. 195, pp. 3523-3528, 2010.
- [3] E. Kjeang, B. T. Proctor, A. G. Brolo, D. A. Harrington, N. Djilali, and D. Sinton, "High-performance microfluidic vanadium redox fuel cell," *Electrochimica Acta*, vol. 52, pp. 4942-4946, 2007.
- [4] S. Hasegawa, K. Shimotani, K. Kishi, and H. Watanabe, "Electricity generation from decomposition of hydrogen peroxide," *Electrochem. Solid-State Lett.*, vol. 8, pp. A119-A121, 2005.

- [5] E. Kjeang, A. G. Brolo, D. A. Harrington, N. Djilali, and D. Sinton, "Hydrogen peroxide as an oxidant for microfluidic fuel cells," *J. Electrochem. Soc.*, vol. 154, pp. B1220-B1226, 2007.
- [6] D. D. Meng and C.-J. Kim, "An active micro-direct methanol fuel cell with self-circulation of fuel and built-in removal of CO₂ bubbles," *J. Power Sources*, vol. 194, pp. 445-450, 2009.
- [7] C. Y. Chen and P. Yang, "Performance of an air-breathing direct methanol fuel cell," *J. Power Sources*, vol. 123, pp. 37-42, 2003.
- [8] S. Ha, B. Adams, and R. I. Masel, "A miniature air breathing direct formic acid fuel cell," *J. Power Sources*, vol. 128, pp. 119-124, 2004.
- [9] E. R. Choban, L. J. Markoski, A. Wieckowski, and P. J. A. Kenis, "Microfluidic fuel cell based on laminar flow," *J. Power Sources*, vol. 128, pp. 54-60, 2004.
- [10] T. I. Valdez, S. Narayanan, C. Lewis, and W. Chun, "Hydrogen peroxide oxidant fuel cell systems for ultraportable applications," *Proc. of the Int. Symp. DMFC*, vol. 4, pp. 265-273, 2001.

CHAPTER 5

COMBINED FULL FUEL CELL

At last, but not the least, in this chapter we combine and integrate the two components described in Chapters 2 and 4, i.e., self-pumped anode and self-regulated oxygen supply in cathode, into a full fuel cell, to realize a *stackable miniature fuel cell with on-demand fuel and oxygen supply*, the title of this dissertation.

5.1 Introduction

Our approach in developing miniature fuel cells is to systematically eliminate all the ancillary components required for fuel cell operation in order to remove the packaging penalty and realize true miniaturization of fuel cell for portable applications. A self-regulated operation, i.e., consuming the fuel only when there is an external load without a discrete unit for sensing and feedback, would be an ideal design. Furthermore, our objective is to develop stackable unit fuel cells for scale up applications.

So far, we introduced how we have successfully eliminated major ancillary components in anode and channel compartment, liquid fuel pumps and gas separators and oxygen tanks, by designing bubble pumping mechanism inside the channel and employing an air-breathing cathode. We have also noted the air-breathing cathode limits the fuel cell from high power applications, for which stacking of the fuel cells is most likely needed, and addressed the issue by designing a self-regulated generation of oxygen on board [1].

With the fuel self-pumping and oxidant self-generation combined together in a single device, the device is no longer dependent on the ancillary components or the environment around the fuel cell. Since fuel does not need external instrument for pumping, the fuel cell is truly portable; and since the cathode does not need to breathe oxygen from air, the unit fuel cells can be stacked for higher power output. Standalone with no moving part and no interconnect, the simple construction of liquids in solid containers makes the resulting fuel-cell system truly scalable.

5.2 Mixed potential issue on oxygen generating plate

In order to integrate the oxygen-generating structure of Chapter 4 as a cathode in a full fuel cell, we came up with a first generation design as shown in Fig. 5-1. The oxygen is directly supplied to cathode while self-pumping of fuel occurs in the anodic chamber. Ionic conduction of H^+ ion between anode and cathode is performed by small opening connection with help of Nafion membrane in between for better separation and less mixing. However, when the oxygen supply was integrated, current configuration of a cathode structure had to serve as both oxygen generation (giving electron) and consumption (receiving electron). In this design, unfortunately, the issue of mixed potential turned out to be unavoidable.

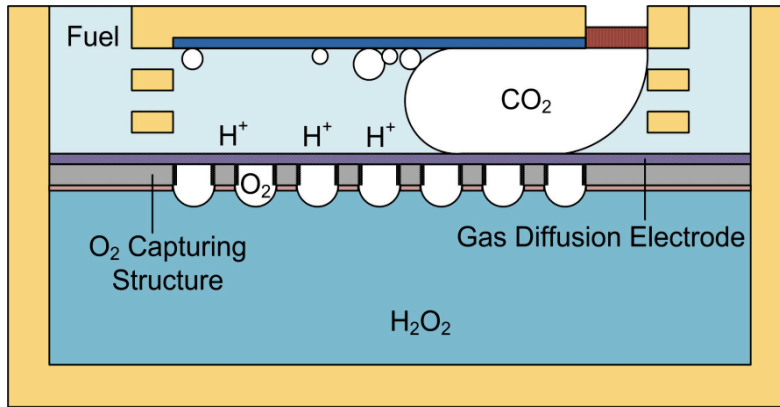
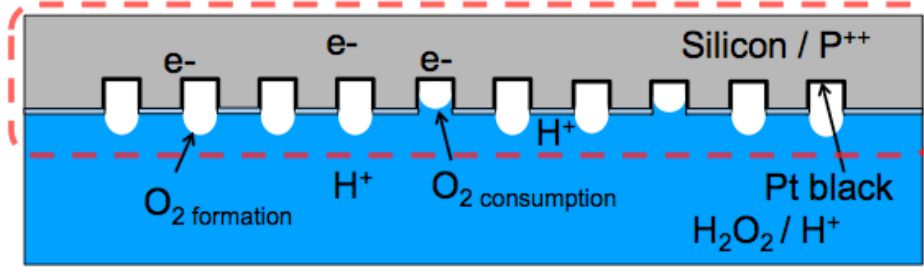
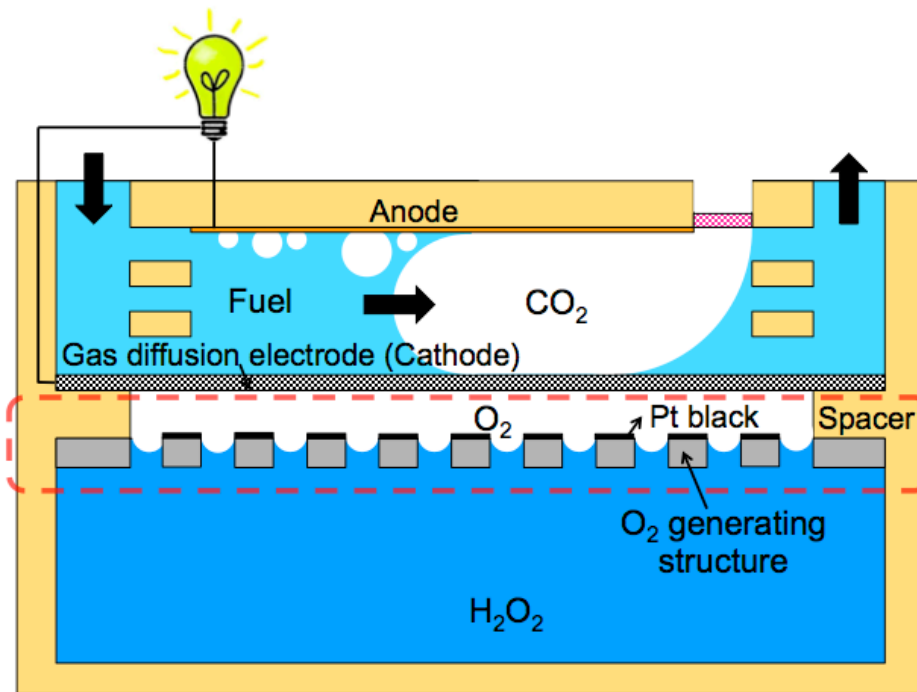


Figure 5-1: Preliminary (1st generation) design of combined full fuel cell. Cathode generates and consumes O_2 on board and anode self-pumps the fuel from fuel reservoir.

In order to address the mixed potential issue, we developed a new design that separates the oxygen generation from the oxygen consumption on the cathode. Figure 5-2(b) [2] explains the mechanism of the current design, modified from the previous version (Fig. 5-2(a) or Fig. 5-1) [1]. A silicon-based oxygen generating structure is set some distance away from the cathode by a spacer to blanket the backside of air-breathing cathode with a layer of oxygen. In this way, gas diffusion electrode (i.e., cathode) is in direct contact and provided with high concentration of oxygen so that the oxygen deficient issues in the stacked fuel cells are solved. More importantly, the mixed potential issue is solved since hydrogen peroxide decomposition (i.e., electron giving) and oxygen reduction (i.e., electron receiving) are occurring at their designated structures.



(a)



(b)

Figure 5-2: Schematic design of (a) previously reported design [1] compared to (b) the full fuel cell combining the self-regulated oxygen supply directly on cathode of self-pumping fuel cell [2].

5.3 Mechanism

Instead of having micropockets, current design consists of hydrophilic through holes to wick catholyte (30% hydrogen peroxide) to the catalyst (Pt black) surface, where hydrogen peroxide is decomposed into oxygen. Once the gap between the oxygen-generating structure and cathode is filled with oxygen gas, the catalyst is covered with the gas and ceases to generate more oxygen until it is consumed to expose catalyst to hydrogen peroxide containing catholyte.

In this new design, the Pt catalyst on O₂ generating structure and gas diffusion electrode (GDE) have different roles. Unlike other hydrogen peroxide utilizing fuel cells, cathode catalyst on GDE does not face hydrogen peroxide but face just the decomposed oxygen. Catalyst on O₂ capturing structure first sees the hydrogen peroxide, and decomposition starts. O₂ bubble blocks the bulk H₂O₂ from cathode catalyst so that no mixed potential due to decomposition occurs on the cathode. In other words, the cathode reduces O₂ into water, completing the fuel cell reaction, while O₂ generating structure decomposes H₂O₂ into O₂ and provides the pure gaseous O₂ to cathode.

5.4 Structure design of hydrogen peroxide DFAFC with self-pumping of fuel

Fabrication of the integrated fuel cell system is relatively simple compared with existing micro fuel cells due to its simple structures without moving parts. The active part of the device was machined into a piece of chemically inert plastic, such as polycarbonate, using a computer numerical control (CNC) milling machine. This is similar to the air-breathing self-pumping fuel cell introduced in Chapter 2.

As a proof-of-concept device, the developed O₂ generating plate, which is modified from the design introduced in Chapter 3, has been attached to the bottom of the existing air-breathing fuel cell to directly supply O₂. The fabrication method of O₂ generating plate is similar but slightly modified.

5.5 Fabrication of designed full fuel cell

The fabrication of oxygen-generation structure has become simpler because there is no need to deposit platinum black inside the pockets anymore (Fig. 5-3 vs. Fig. 4-3 of [10]). Previously, in order to deposit Pt black inside the micropockets, uniform coating of gold seed layer was important before the platinum-plating step. Also vacuuming the structure before the electroplating was important to remove the air trapped inside the structure and to ensure that the plating solution wets the pockets for reliable plating process. In comparison, in the current design we only need platinum black on the top side of the structure, making the process much simpler and more reliable. Starting with a 4” silicon wafer (500 mm thick), we first deposited and patterned a 3 μm silicon dioxide into arrays of 100 μm holes with 200 μm pitch to mask the subsequent DRIE. After through-hole etching by DRIE, the wafer was thoroughly cleaned and thermally oxidized. The oxidation enables the through-holes of the structure to wick the hydrogen peroxide through the holes to the Pt black on the other side by its hydrophilic nature. After evaporating 20/200 nm Cr/Au seed layer, we electroplated a high surface area Pt black on a defined area at 1 A/cm² for 10 seconds for rigorous hydrogen peroxide decomposition. The plating solution was prepared by mixing 1 gram of chloroplatinic acid (Sigma Aldrich) into 100 mL of DI water and 30 mL of lead acetate (Sigma Aldrich).

Since the microstructures do not serve as a cathode anymore, the silicon wafer does not need to be highly conductive (as used in [1]) anymore. Furthermore, in case of mass manufacturing, the structure made by the fourth step in the process flow can be simply replaced with a porous glass slide, leaving only Cr/Au deposition and Pt black electro-deposition.

The fabricated oxygen-generating structure is shown in Fig. 5-4. The images on the left column show the topside of the structure facing a gap for cathode, indicated in Fig. 5-3. The shape of the plated Pt black area is determined to match the shape of the channel for bubble pumping. The bottom side is a thermal oxide for hydrophilic structure, where it faces the catholyte with hydrogen peroxide. Successful Pt black deposition with high surface area was checked under the microscope.

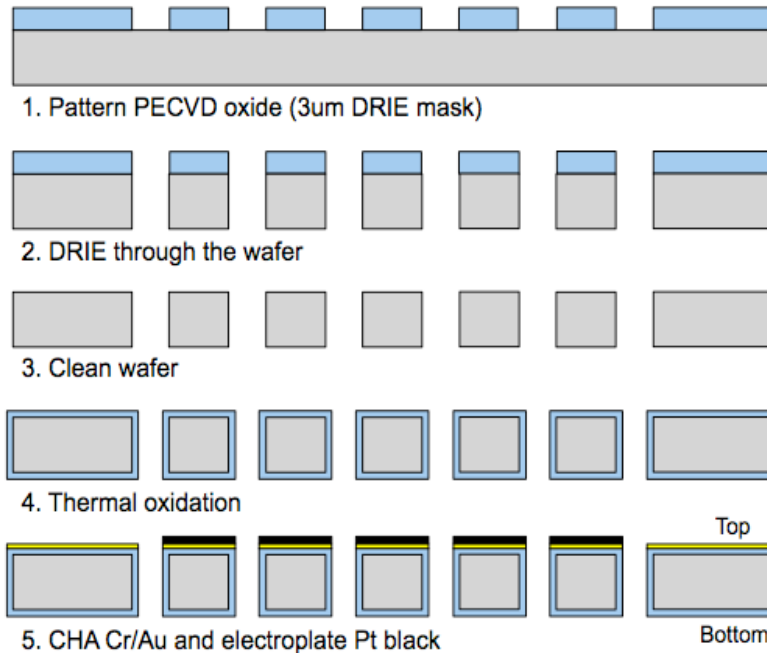


Figure 5-3: Process flow to fabricate oxygen generating structure with hydrophilic through holes for slow supply of hydrogen peroxide. Platinum black is electroplated for hydrogen peroxide decomposition.

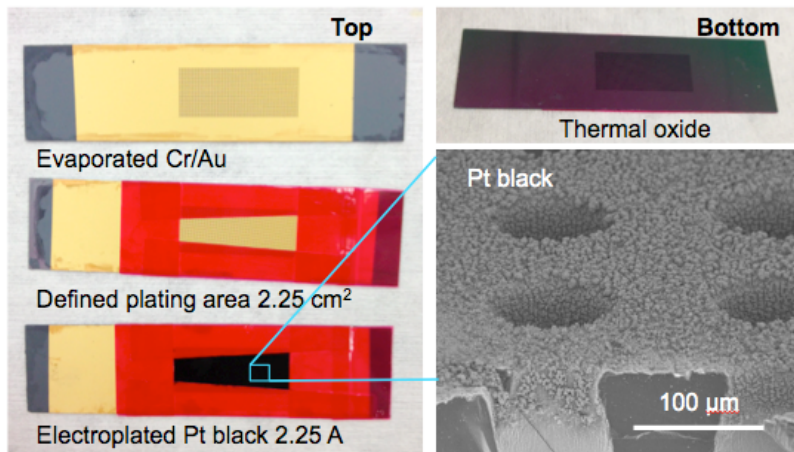


Figure 5-4: Images of fabricated oxygen generating structure. Top surface (indicated in Fig. 5-3) has Pt black in a shape corresponding to the cathode, and bottom surface has thermally grown oxide for hydrophilic wetting of hydrogen peroxide inside the holes.

Finished components of a fuel cell and a fuel cartridge are mated, and a nanoporous venting plug fills the venting hole. Assembly is expected to be relatively easy, since there are no delicate membranes (e.g. MEA), which would have required a careful but strong clamping to prevent leaking. Since the defined structures in anodic and cathodic chamber regulate the supply of fuel and oxygen source within themselves, the system will be very small in size after miniaturization (< 1 cm) including the fuel and hydrogen peroxide storage (Fig. 5-5).

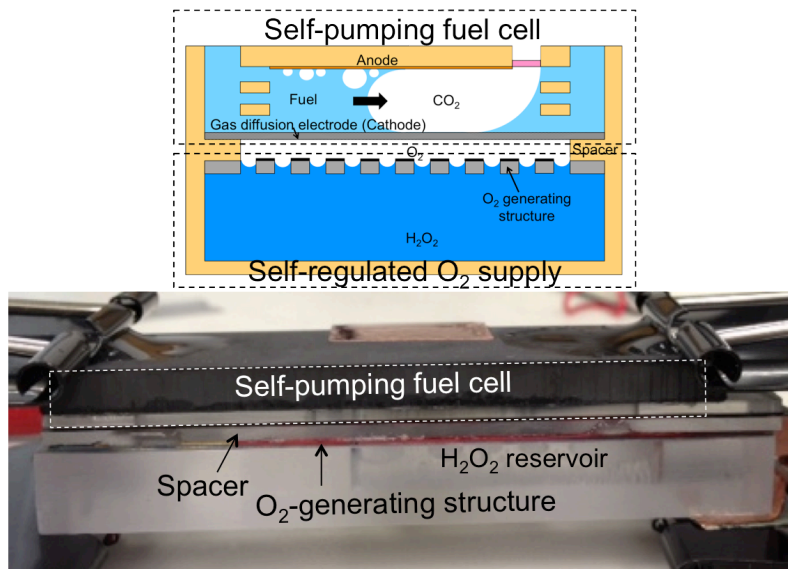
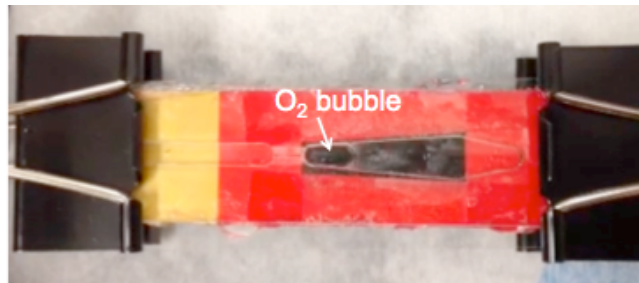


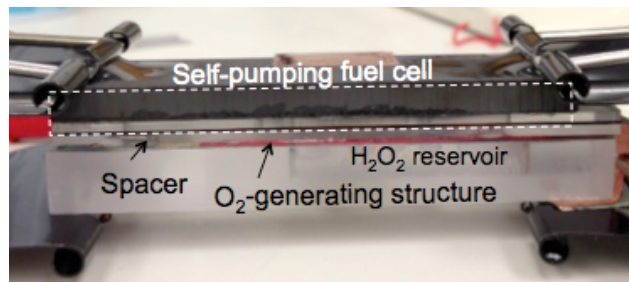
Figure 5-5: Assembled full fuel cell with self-pumping anode and self-regulated O_2 supply integrated in one device.

5.6 Experimental setting

The effect of oxygen generation from the fabricated structure has been tested by assembling the O₂-generating structure onto a hydrogen peroxide reservoir and placing a glass slide above the O₂-generating structure (Fig. 5-6(a)). In other words, the air-breathing fuel cell part was removed from full fuel cell assembly to observe the oxygen generation. A glass slide was placed on top of the spacer for easy visualization. The spacer placed between the O₂-generating structure and the glass slide formed a gap to collect and provide O₂ directly under the cathode. The result has been observed from the top through the glass slide, monitoring the oxygen layer being created and gradually dewetting the spacer gap.



(a)



(b)

Figure 5-6: Picture of (a) oxygen bubble filling the gap between the oxygen generating structure and a glass slide on top (top view), and (b) oxygen generating structure assembled with self-pumping fuel cell for direct oxygen supply to the cathode (side view).

Furthermore, we made a preliminary testing setup of a full fuel cell by assembling the oxygen supply below the self-pumping fuel cell with air-breathing cathode [3], so that the fuel cell runs with a direct supply of oxygen generated from the structure (Fig. 5-6(b)). Fuel cell testing was performed with and without the oxygen generating structure attached on the bottom of cathode. The testing was monitored using Keithley 2400 power supply connected to a computer to record the current and voltage output from our full fuel cell.

5.7 Testing of integrated fuel cell

5.7.1 Testing of oxygen generation

In the first preliminary testing of oxygen supply in the fabricated structure (Fig. 5-6(a)), the air-breathing fuel cell part was removed to observe the oxygen generation. A glass slide was placed on top of the spacer for easy visualization. Figure 5-7 shows the viewing direction of the snapshots displayed within the figure.

Rigorous oxygen generation and quick gas filling (~9 mL/min) of the gap have been observed using 7.5% hydrogen peroxide in DI water. Oxygen generation ceased for a while after the gas filled the gap completely so the Pt is fully dewetted. However, after a while the O₂ accumulated inside the gap between the plates seemed to have leaked through the seal, resulting in the beginning of next cycle of rigorous oxygen generation. For a self-regulated oxygen generation system, sealing of the oxygen-filled gap is of great importance. If the generated oxygen leaks between the plates, the next cycle of hydrogen

peroxide wicking would occur to waste the stored hydrogen peroxide, i.e., the oxygen source, during the storage stage.

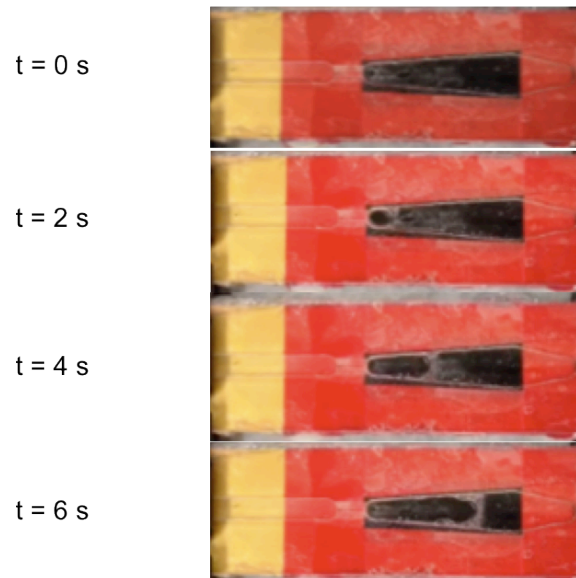
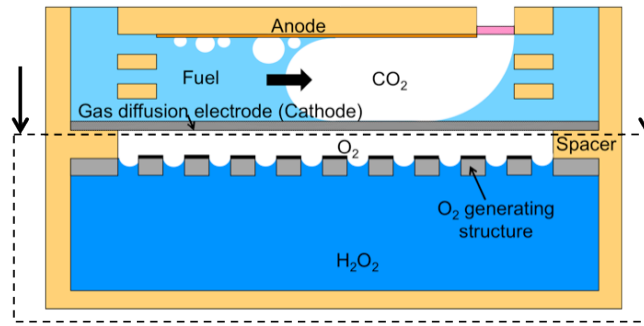


Figure 5-7: Snapshots of rigorous O₂ generation during testing of oxygen supply half of the fuel cell system without fuel supply system. Glass slide is placed on top of spacer to seal the gap and provide clear visualization of oxygen bubbles filling the gap.

5.7.2 Testing of combined full fuel cell

Current density of three different cases of operation was tested for verifying the viability of full fuel cell. When fuel cells are stacked, we anticipated that the oxygen delivery to the cathode would be limited and the current density lowered. We have blocked the cathode of air-breathing fuel cell to simulate a stacked configuration of multiple air-breathing fuel cells. As predicted, the current density output was significantly lower than the single (i.e., not stacked) case that the pumping was not effective anymore. Although very low, there was still some current output due to leakage of oxygen through the gap between the assembled layers. This test verified that when air-breathing fuel cells are stacked for higher power output, the performance will drop due to lack of oxygen delivered to the cathode.

On the other hand, when oxygen-generating structure with H_2O_2 reservoir is attached to the bottom of cathode, the high current density output of air-breathing case is recovered with rigorous pumping in the anodic channel and oxygen generation in the cathodic chamber (Fig. 5-8).

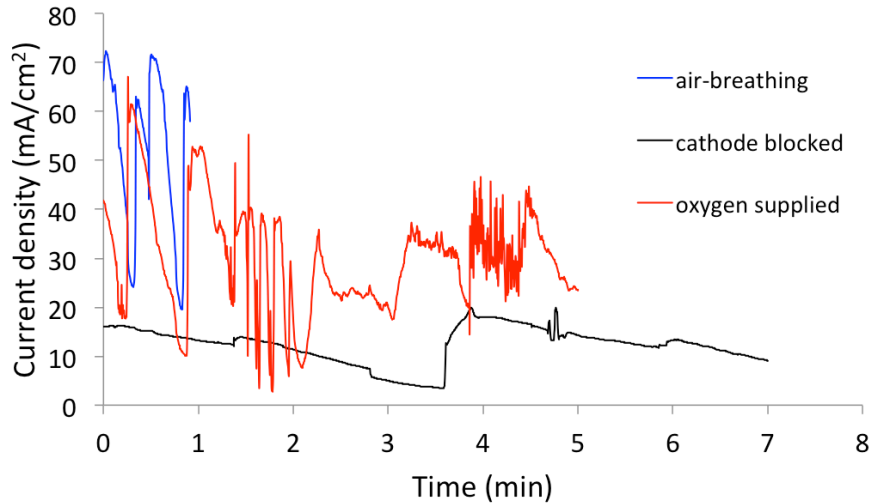


Figure 5-8: Current density of three different cases of operation. When cathode is blocked from air-breathing fuel cell to simulate stacked condition, current density drops significantly due to lack of oxygen delivered to cathode. On the other hand, the combined full fuel cell with oxygen generated on chip has shown to recover the current density of air-breathing fuel cell case.

5.7.3 OCP of combined full fuel cell

OCP of full fuel cell and air-breathing fuel cells were tested and compared. Air-breathing fuel cell shows stable OCP around 0.5 V with little fluctuation along time. On the other hand, developed full fuel cell shows fluctuating but occasionally higher OCP reaching 0.7 V. High OCP can be explained by direct O₂ supply with some pressure inside enclosed cell. Occasional low OCP can be by the low pressure in O₂ due to the usage and leakage. When fully developed with better sealing technology and fast oxygen supply, the OCP of full fuel cell will always stay higher than air-breathing fuel cell.

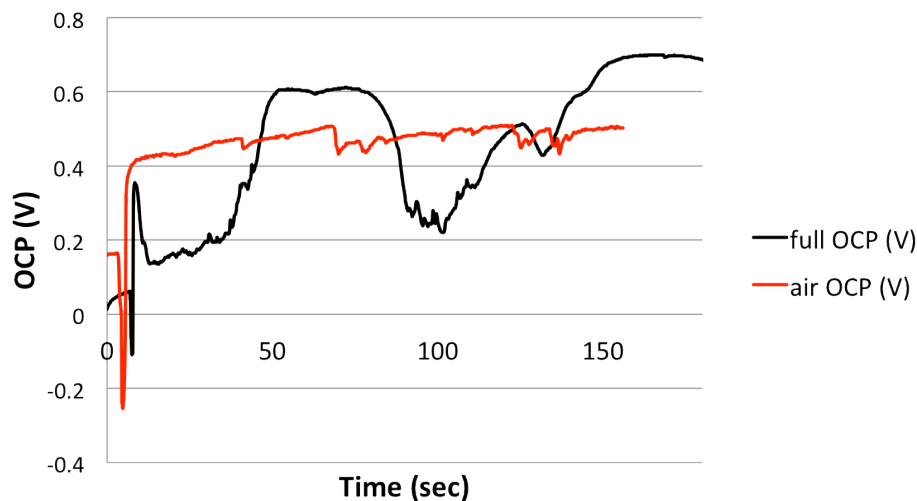


Figure 5-9: OCP of full fuel cell and air-breathing fuel cells. While air-breathing fuel cell case shows stable OCP around 0.5 V, full fuel cell shows fluctuating but occasionally higher OCP reaching 0.7 V. High OCP can be explained by direct O₂ supply with some pressure inside enclosed cell.

5.7.4 Performance curve of combined full fuel cell

We have also checked the performance curve of both cells, an air-breathing case and an oxygen supply case, respectively. In the air-breathing case, we obtained fuel cell output of 17.4 mW/cm² maximum power density at 0.25 V and 0.5 V OCP, which are similar to the previously reported data [3]. This step also provided verification of the fabricated fuel cell before attaching the self-limiting oxygen supply system (Fig. 5-10).

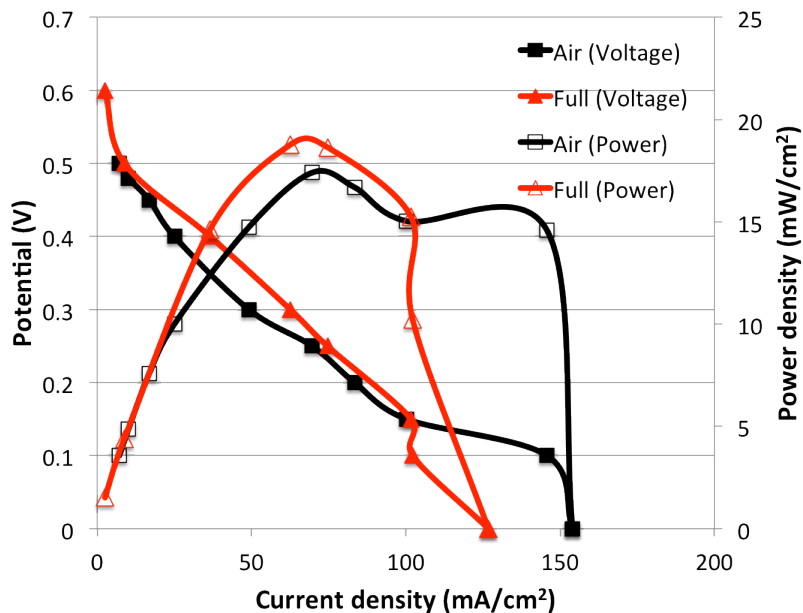


Figure 5-10: Polarization curve drawn from the integrated full fuel cell compared with the air-breathing full fuel cell.

The fully assembled fuel cell with active oxygen supply on the bottom of GDE showed similar performance in the polarization curve (Fig. 5-10). The maximum power density of 18.8 mW/cm^2 was obtained using the same device. Not only the power density was similar but also the OCP was raised to 0.6 V when high concentration oxygen with some pressure was supplied directly to the GDE rather than 20 % of oxygen breathed in from the ambient air.

5.7.4 Longer pumping of fuel cell

A longer pumping of the developed fully integrated fuel cell was operated with 5 mL of fuel in the fuel reservoir and 1.5 mL of 30 % H_2O_2 stored in the oxidant reservoir. The fuel cell was operated under 0.2 V, which is close to the voltage at which the cell

shows peak power density. Under the external load, the full fuel cell operated with a steady self-pumping until the oxidant from the reservoir was depleted.

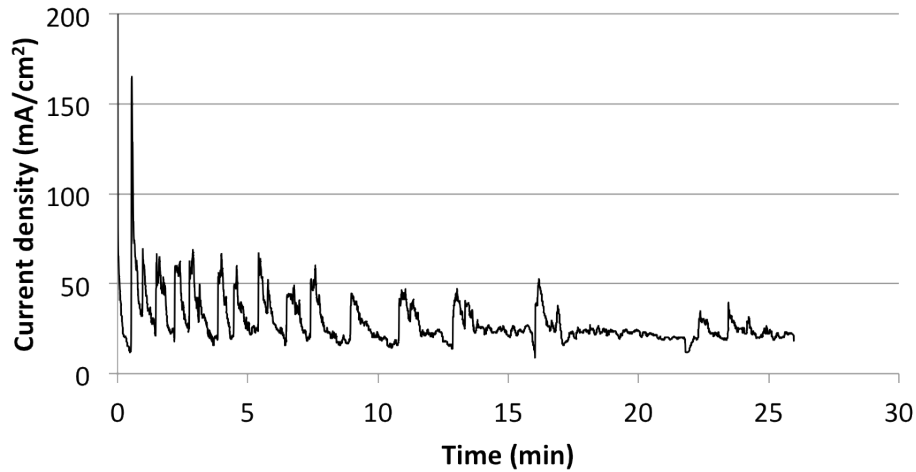


Figure 5-11: Fully integrated fuel cell was operated for longer term. While fuel was supplied, fuel cell operated with steady pumping until the oxygen from H_2O_2 reservoir was depleted.

Utilization of hydrogen peroxide was seen to be 1 - 2.5 %, which is very low. Majority of the oxidant was wasted in the beginning stage where oxygen generation was vigorous because the assembly was not sealed. Also, in the beginning of the fuel cell operation, the pressure of oxygen gas in spacer area was high enough to pass through air-breathing cathode and pump the fuel channel for some time until the pressure was moderate enough for CO_2 pumping with no O_2 penetration. The gas leakage problem in the cathodic chamber during assembly before testing will be reduced when prototype resembling final product is developed, since the device can be assembled firmly for permanent packages. Furthermore, the oxygen penetration issue can be addressed by

carefully designing O₂-generating chamber with optimized concentration of hydrogen peroxide.

Although additional improvements are need to reduce wasting generated oxygen, the result conveys that the implementation of active oxygen generation directly to the cathode enables the stacking of the fuel cells while maintaining the power output. This issue is alleviated by providing near pure gaseous oxygen supply to the cathode in confined area and balancing the fuel cell reaction.

5.8 Conclusion

We have been continuing our effort to realize a full fuel cell without any ancillary component. The recently reported self-regulated oxygen generation has been modified to integrate in a full fuel cell. The preliminary results confirmed the feasibility of the proposed approach. The simple yet powerful fuel cell of a simple liquid-in-container construction, i.e., free of any ancillary or moving component, makes the miniature fuel cell self-sustainable in a small volume compared with the existing design that requires a mechanical pump and a hydrogen gas tank or a reformer. Furthermore, elimination of the need to access air for oxygen breathing suggests that the miniature fuel cell may be configured stackable for higher power demands in the future.

References

- [1] Hur J. I. and Kim C.-J. 2012 A micrstructured cathode for fuel cell with self-regulated O₂ creation and consumption *Proc. Conf. MEMS, (Paris, France, January 2012)* 35-38.
- [2] Hur J. I. and Kim C.-J. 2012 Self-contained oxygen supply for self-regulating miniature fuel cell *Proc. Conf. powerMEMS, (Atlanta, Georgia, December 2012)*.
- [3] Hur J. I., Meng D. D. and Kim C.-J. 2011 Self-pumping membraneless miniature fuel cell with an air-breathing cathode *J. MEMS*, **21** 476-483.

CHAPTER 6

CONCLUSION & OUTLOOK

Our series of efforts in developing miniature power sources is summarized by introducing idea, design, fabrication and testing all in one context: to develop a miniature fuel cell that meets the need in longer-lasting miniature power sources for ever energy hungry portable consumer electronics.

A miniature fuel cell equipped with self-pumping of fuel and self-regulated oxygen generation has been realized as a whole system without any help from ancillary components. The results showed the feasibility of our proposed mechanisms and demonstrated the integration of them as a full fuel cell. The simple yet powerful fuel cell of a liquid-in-container construction makes the miniature fuel cell self-sustainable in a small volume. We have also developed a micromachined fuel cell for millimeter-scale applications, verifying that further scaling down of fuel cell is simply done by structuring the solid components in smaller scale without the “packaging penalty”. Further elimination of the need to access air for oxygen breathing suggests that the miniature fuel cell may be configured stackable for higher power demands in the future.

6.1 Summary

We were able to realize:

6.1.1 Stackable fuel cell

Without the need to access the oxygen in the surrounding air, the developed design is stackable to generate higher power for scale up applications. Decomposed oxygen from hydrogen peroxide in cathodic chamber is always ready for use.

6.1.2 Balanced anodic and cathodic reaction

Removing the limitation of oxygen supply common in most of the current micro fuel cells, the proof-of-concept device significantly increased the oxygen reduction rate and improved the fuel cell performance. Furthermore, since the oxygen deficiency is resolved, higher concentration fuels (e.g. methanol or formic acid) can be used to further enhance the fuel-cell performance.

6.1.3 A standalone system of liquid-in-container construction

One of the important benefits of the developed fuel cell is that it is comprised of only solid structures that contain active liquids (i.e., fuel and oxidant) and no moving elements. All the necessary functions, which the multiple ancillary components in the normal fuel cells provide, are now all embedded in the microfluidic mechanisms of the miniature fuel cell: pumping of the fuel, removal of the byproduct CO₂, and supply of the oxygen.

6.1.4 High energy density and high power density

Due to the simple design of our system without dead volumes occupied by the ancillary components, more space is dedicated to energy storage, leading to higher energy density, i.e., more energy per unit volume of the system. Also, parasitic power loss to operate the fuel pump is eliminated, since bubble pumping spontaneously starts and stops when fuel-cell circuit is closed in need of electricity and open when the need is over. Similarly, oxygen generation is self-regulated so that there is no need to run the oxidant pump or opening and closing a valve of oxygen tank to supply oxygen.

6.1.5 Flexible choice of fuel-electrolyte

As long as the fuel and electrolyte are compatible with hydrogen peroxide and the fuel produces gaseous byproduct as a result of oxidation, the proposed design is in principle valid for any choice of fuel and electrolyte. The conditions of the fuel and electrolyte—such as pH—can be tailored to achieve higher kinetics.

6.1.6 Easy scaling down or scaling up

Further miniaturization or scale up design is simpler by eliminating the packaging penalty. The solid structures of the fuel cell can be simply scaled up or down as far as manufacturable. The manufacturing methods can be developed and improved to lower the cost of fuel cell, expand the size range of the fuel cell, etc.

6.2 Outlook

Currently, the project has reached the stage that all the key mechanisms have been verified and full fuel cells demonstrated. Improvements in current fuel cells can be achieved to further increase energy density of developed fuel cells by: (1) developing fuel concentration regulation system on board to store high concentration fuel in cartridge, and (2) developing a fuel cell with novel catalyst that will significantly reduce the problem of catalyst deactivation in current state-of-art fuel cells. After this, efforts may be put in to improve the fuel-cell performances for eventual commercialization. In order to step forward, developing a prototype resembling a consumer product is required to help identifying next key issues. With the prototype, the actual efficiency and fuel utility can also be achieved to compare with existing power sources.

6.2.1 Concentration regulation

Most fuel cells operate at a reduced concentration of their fuel typically at 5-10 vol% for MEA-based fuel cells. As the fuel is diluted, its high energy density is compromised. To minimize this drawback, an effective fuel concentration regulator is desired to reduce the amount of solvent (water) stored in the system. An effective fuel dilution mechanism that allows storage of high concentration fuel is a key component to significantly increase the overall energy density of the fuel cell chip.

6.2.2 Minimizing catalyst deactivation

Currently available state-of-art microfluidic fuel cells suffer from low fuel utilization due to catalyst deactivation or CO-poisoning. In order to increase the fuel utilization and ultimately energy density, many efforts are being made to reactivate the surface by applying reverse potential [1]. Incorporating proper reactivation technology into miniature fuel cells, or developing novel catalyst that will stay active during fuel cell operation is essential in realizing high energy density fuel cells that will outperform batteries.

6.2.3 Prototype fuel-cell stack

A prototype fuel-cell stack is perceived as shown in Figure 6-1. A fuel cell is comprised of an anodic channel filled with a fuel and a cathodic chamber filled with hydrogen peroxide, and a cartridge attached to the fuel cell. A leak-proof venting structure is plugged in the fuel-cell stack to vent out the carbon dioxide bubbles produced and used in anodic channel for fuel pumping. One compartment of the cartridge stores fuel and is connected to the inlet and outlet of the anodic channel. The other compartment of the cartridge stores hydrogen peroxide and is connected to the cathodic chamber. When the fuel or hydrogen peroxide is depleted below an acceptable concentration, the cartridge will be detached and filled up with a fresh fuel and hydrogen peroxide or simply replaced with a new cartridge.

The fuel cell is insensitive to the gravitational orientation, because the feature sizes of all the key fluidic components are below a millimeter, where surface tension dominates over gravity. Structural material can be selected from a wide range of materials as long as they are mechanically robust, machinable, and chemically inert to the fuel and hydrogen peroxide.

Figure 6-1 shows how the fuel cells may be stacked ultimately. A vent plug for the carbon dioxide is placed in the middle, and several channels integrated inside the packaging shell are oriented in the way the hydrophobic vents are positioned in the middle. Figure 6-1 (b) shows how the channels are laid out. Electrical connection of the fuel cells are drawn outside of the package and made able to plug into another cell when stacked (Fig. 6-1a & 6-1c)). Depending on how users want to connect the fuel cell, either in parallel or series, or in both ways, they can define which orientation to plug. Figure 6-1(c) is a diagram showing a stack of eight fuel cells, two cells in series multiplied to four in parallel.

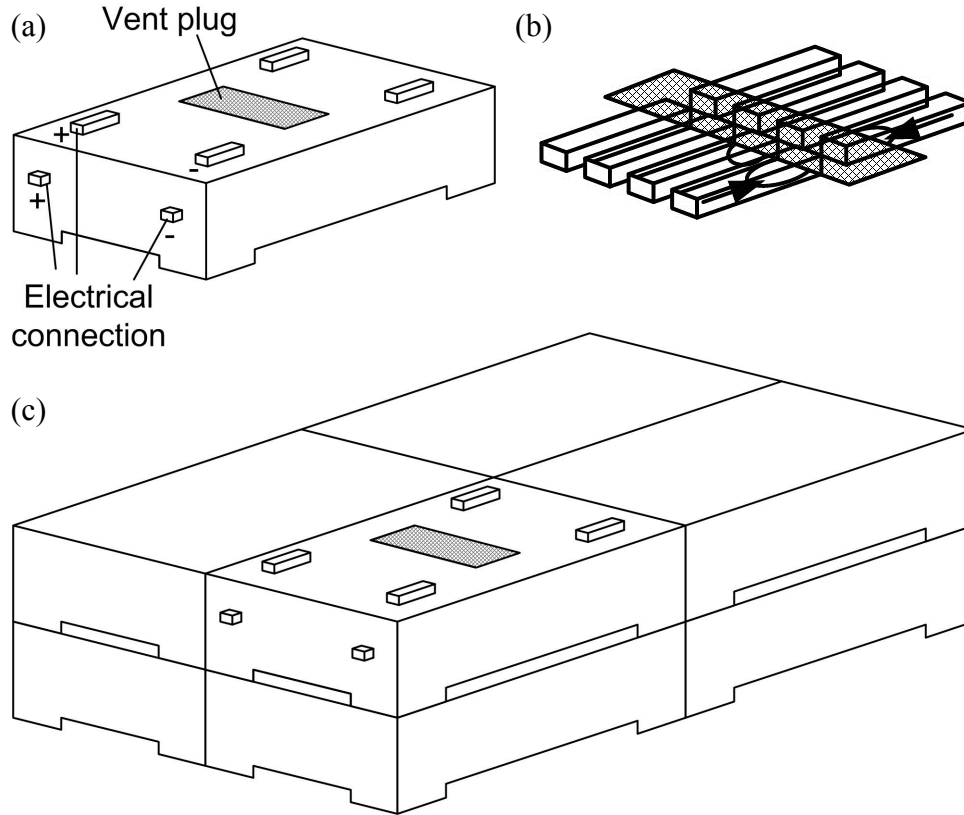


Figure 6-1: Schematic drawing illustrating the proposed fuel cells for stacking. Each fuel cell has electrical connections and vent plug. The figure is not drawn to scale.

6.2.4 Micromachined smaller fuel cells

Figure 6-2 shows a schematic drawing of further miniaturized version of the developed all-inclusive fuel cell with the cartridges. As introduced in Chapter 3, the micromachined fuel cell will be further integrated with oxygen source and packaged. Fuel cartridge can be designed in several different ways to explore the best scenario for refueling for the case whether a single fuel cell chip is used or stacked.

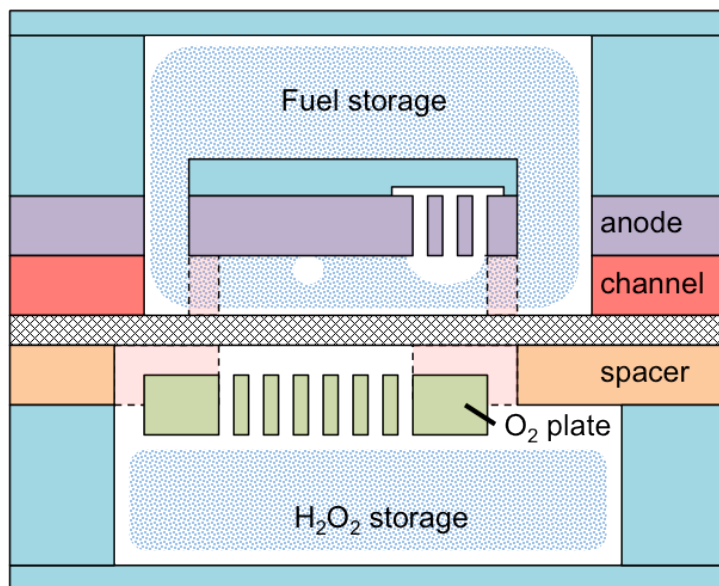


















Figure 6-2: Schematic drawing illustrating the integrated micro fuel cells for stacking.

6.2.5 Estimated performance

Due to the higher specific energy of their fuels compared with batteries, fuel cells can have a higher energy density than batteries in theory. Free from ancillary components, which penalize the packaging in small scale, and also free from the MEA, the miniature fuel cell chip is expected to maintain much of the high energy density inherent in its concentrated fuel. Using a less amount of solids, the fuel cell chip is also expected to weigh less than batteries. Assuming a full utilization, the energy capacity and weight of the fuel cells are estimated in Table 6-1 in reference to the volumes of two common commercial batteries: AAA and CR2032 button-cell. For the calculation, the housing structures were assumed to occupy 10% of total volume of the fuel cell, leaving the remaining 90% for the active fluids. For a DMFC chip, the active fluids are expected to be 67.5% H_2O_2 and 22.5% methanol. For DFAFC, they are expected to be 45% H_2O_2

and 45% formic acid. According to the calculated values in Table 6-1, the fuel cell chips are estimated to weigh less and provide more energy compared to the existing commercial batteries [2-4]. Our first goal in the commercialization of this technology will be to achieve the weight and energy capacity comparable to the lithium-ion batteries, with a room spared for future improvement to gradually find its killer application in the market and finally replace the batteries in the near future.

Table 6-1: Comparison of weight and energy capacity between existing batteries and developed fuel cell chips. In developed fuel cell chip with methanol and formic acid fuel, weight is greatly reduced and superior energy capacity is available.

Battery Type (Volume)	Power Source		Weight (g)		Energy Capacity (mAh)	
AAA (3.85 cm ³)	Battery	Alkaline		11.5		750
		NiMH		14.5		950
		Lithium		7.6		1200
	Fuel-cell chip	DMFC		4.9		3440
		DFAFC		9.3		2460
CR2032 (1.01 cm ³)	Battery	Lithium		3.2		240
	Fuel-cell chip	DMFC		1.3		900
		DFAFC		2.5		645

References

- [1] X. Yu, P.G. Pickup, “Deactivation/reactivation of a Pd/C catalyst in a direct formic acid fuel cell (DFAFC): Use of array membrane electrode assemblies,” *Journal of Power Sources*, vol. 187, pp. 493–499, 2009.

[2] “Button Cell,” https://en.wikipedia.org/wiki/Button_cell

[3] “List of battery sizes,” http://en.wikipedia.org/wiki/List_of_battery_sizes

[4] “Battery (electricity),”

http://en.wikipedia.org/wiki/Battery_capacity#Capacity_and_discharging